Intercepting the Lipid-Induced Integrated Stress Response Reduces Atherosclerosis

Umut I. Onat, BSc,[a,b] Asli D. Yildirim, MSc,[a,b,c,d] Özlem Tufanli, PhD,[a,b] Ismail Çimen, PhD,[a,b] Begüm Kocatürk, PhD,[a,b,e]
Zehra Veli, MSc,[a,b] Syed M. Hamid, PhD,[c,d] Kenichi Shimada, PhD,[c,f,g] Shuang Chen, MD, PhD,[c,g,h] Jon Sin, PhD,[c,d]
Prediman K. Shah, MD,[d,f] Roberta A. Gottlieb, MD, PhD,[c,d] Moshe Arditi, MD,[c,d,g,h] Ebru Erbay, MD, PhD[a,b,c,d]

ABSTRACT

BACKGROUND Eukaryotic cells can respond to diverse stimuli by converging at serine-51 phosphorylation on eukaryotic initiation factor 2 alpha (eIF2α) and activate the integrated stress response (ISR). This is a key step in translational control and must be tightly regulated; however, persistent eIF2α phosphorylation is observed in mouse and human atheroma.

OBJECTIVES Potent ISR inhibitors that modulate neurodegenerative disorders have been identified. Here, the authors evaluated the potential benefits of intercepting ISR in a chronic metabolic and inflammatory disease, atherosclerosis.

METHODS The authors investigated ISR's role in lipid-induced inflammasome activation and atherogenesis by taking advantage of 3 different small molecules and the ATP-analog sensitive kinase allele technology to intercept ISR at multiple molecular nodes.

RESULTS The results show lipid-activated eIF2α signaling induces a mitochondrial protease, Lon protease 1 (LONP1), that degrades phosphatase and tensin-induced putative kinase 1 and blocks Parkin-mediated mitophagy, resulting in greater mitochondrial oxidative stress, inflammasome activation, and interleukin-1β secretion in macrophages. Furthermore, ISR inhibitors suppress hyperlipidemia-induced inflammasome activation and inflammation, and reduce atherosclerosis.

CONCLUSIONS These results reveal endoplasmic reticulum controls mitochondrial clearance by activating eIF2α-LONP1 signaling, contributing to an amplified oxidative stress response that triggers robust inflammasome activation and interleukin-1β secretion by dietary fats. These findings underscore the intricate exchange of information and coordination of both organelles' responses to lipids is important for metabolic health. Modulation of ISR to alleviate organelle stress can prevent inflammasome activation by dietary fats and may be a strategy to reduce lipid-induced inflammation and atherosclerosis. (J Am Coll Cardiol 2019;73:1149–69) © 2019 The Authors. Published by Elsevier on behalf of the American College of Cardiology Foundation. This is an open access article under the CC BY-NC-ND license (http://creativecommons.org/licenses/by-nc-nd/4.0/).

E ukaryotic response to diverse stimuli converges at serine-51 phosphorylation on the eukaryotic initiation factor-2α (eIF2α) and activates an adaptive signaling, the integrated stress response (ISR). This leads to global translation attenuation, but a select group of mRNAs (bearing upstream open reading frames), such as activating transcription factor-4 (ATF4) and CCAT/enhancer-binding protein beta homologous protein (CHOP), continues to be translated. Being a key step for

ABBREVIATIONS AND ACRONYMS

ASKA = ATP-analog sensitive kinase allele

ATF4 = activating transcription factor 4

BMDM = bone marrow–derived macrophages

CCL2 = C-D motif ligand-2

CHOP = CCAT/enhancer-binding protein beta homologous protein

CVD = cardiovascular disease(s)

eIF2α = eukaryotic initiation factor 2 alpha

eIF2B = eukaryotic initiation factor 2B

ER = endoplasmic reticulum

GAS = Group A *Streptococcus*

IL = interleukin

IRE1 = inositol-requiring enzyme-1

ISR = integrated stress response

LONP1 = Lon protease 1

mtROS = mitochondrial reactive oxygen species

NLRP3 = Nod-like receptor family, pyrin domain-containing protein-3

PA = palmitate

Parkin = Parkinson juvenile disease protein 2

PERK = protein kinase R-like endoplasmic reticulum kinase/eIF2α kinase

PINK1 = phosphatase and tensin-induced putative kinase1

SFA = saturated fatty acid

siRNA = silencer RNA

TNF = tumor necrosis factor

UPR = unfolded protein response

translational control, eIF2α phosphorylation must be tightly regulated through dephosphorylation by the protein phosphatase-1 (PP1). In prolonged or severe stress, however, ISR can revert to a cell death program (1,2).

Endoplasmic reticulum (ER) stress is a trigger for ISR. Unfolded proteins are sensed by the ER-resident eIF2α kinase, protein kinase RNA-activated-like ER kinase (PERK), and trigger eIF2α phosphorylation. This homeostatic pathway is hyperactivated in obesity and dyslipidemia (2-4). Evidently, reducing ER stress in mice reduces insulin resistance, obesity, and atherosclerosis (5-8). ER stress is induced by saturated fatty acids (SFA), which are thought to promote cardiovascular diseases (CVD) (9-11). Replacing 5% of the energy intake from SFA with an equivalent intake of monounsaturated fatty acids or polyunsaturated fatty acids is associated with a reduced risk (15% and 25%, respectively) of CVD (12). A causal relationship between SFA intake and CVD risk was demonstrated in nonhuman primates (11). Other studies have challenged SFA's role in human CVD, and the molecular mechanisms of SFA-induced inflammation in atherosclerosis are not completely understood (10).

Increased cellular lipid influx negatively impacts organelles leading to ER and mitochondrial stress, often intertwined in obesity (13). Organelle stress is causally associated with inflammation and atherosclerosis (14). For example, organelle stress activates the Nod-like receptor family, pyrin domain-containing protein-3 (NLRP3) inflammasome, leading to interleukin (IL)-1β and IL-18 secretion (7,15,16). IL-1β is elevated in plaques and serum during dyslipidemia and drives atherosclerosis (7,17-19).

Persistent ISR activation, as evident by eIF2α and PERK phosphorylation, is observed in atheroma (8). PERK promotes foam cell formation, whereas CHOP deletion in mice reduces atherosclerosis (5,6,8,20). The circumstantial evidence thus suggests that PERK-induced ISR may aggravate atherosclerosis, but can intercepting this homeostatic pathway in a chronic disease provide therapeutic gains? Using small molecules and genetic approaches to modulate multiple ISR nodes, we show lipid-activated PERK induces mitochondrial Lon protease-1 (LONP1). LONP1 degrades phosphatase tensin homolog-induced kinase-1

(PINK1) to suppress mitophagy, thus drives mitochondrial reactive oxygen species (mtROS) production and robust inflammasome activation in lipid-stressed macrophages. Finally, ISR inhibition in vivo can suppress hyperlipidemia-induced inflammation and reduce atherosclerosis progression in mice.

METHODS

GENERAL STUDY DESIGN. Three or more independent replicates were performed for cell-based experiments. Mice were randomly assigned to independent cohorts, and data analysis was performed blind. The only elimination criteria used for mouse studies was based on health. Noted differences in mouse numbers (en face aorta and plaque analysis) is related to technical problems that occurred during sampling before analysis.

MICE STUDIES AND TREATMENTS. C57BL/6.129P2-*Apoe*^{tm1Unc}/J mice (*Apoe*$^{-/-}$ mice; received from Jackson Laboratory, Bar Harbor, Maine, and created by Nabuyo Maeda, University of North Carolina), and C57BL/6.129S4-*Prkn*^{tm1Shn}/J (*parkin*$^{-/-}$ mice; received from Jackson Laboratory and created by Jie Shen, Harvard Medical School) and C57BL/6-eIF2αk3$^{tm2201(G646N,M886A)Arte}$ mice (PERK_ASKA [ATP-analog sensitive kinase allele] mice; received from J.R. Lipford at Amgen, Thousand Oaks, California, and created by Taconic Artemis, Cologne, Germany); G646N/M886A mutations were introduced by Cre-Lox system and bred with *Apoe*$^{-/-}$. *Apoe*$^{-/-}$ mice were injected with GSK2606414 (30 mg/kg/day; Atomole Scientific, Wuhan, China) or trans-ISRIB (1 to 2 mg/kg/day; Cayman Chemical, Ann Arbor, Michigan). PERK_ASKA mice were injected with 4-amino-1-tert-butyl-3-(1-naphthyl)pyrazolo[3,4-d]pyrimidine (1-NAPP1) (60 mg/kg/day; Taconic Artemis). Weight and blood glucose were measured weekly (7,15). The experimental animal ethical care committees at Bilkent University and Cedars Sinai Medical Center approved all animal experiment protocols.

DIETS. Western diet (0.21% cholesterol, 21% fat) was obtained from Ssniff-Spezialdiäten, Soest, Germany (TD.88137/E15721).

RESULTS

ISR REGULATES LIPID-INDUCED INFLAMMASOME ACTIVATION. Lipid stress leads to eIF2α and PERK phosphorylation in macrophages and plaques (5,9,20). Here, we sought to understand the contribution of PERK to SFA-induced inflammasome activation and atherosclerosis. Palmitate (PA)

**FIGURE 1** PERK's Role in Lipid-Induced Inflammasome Activation
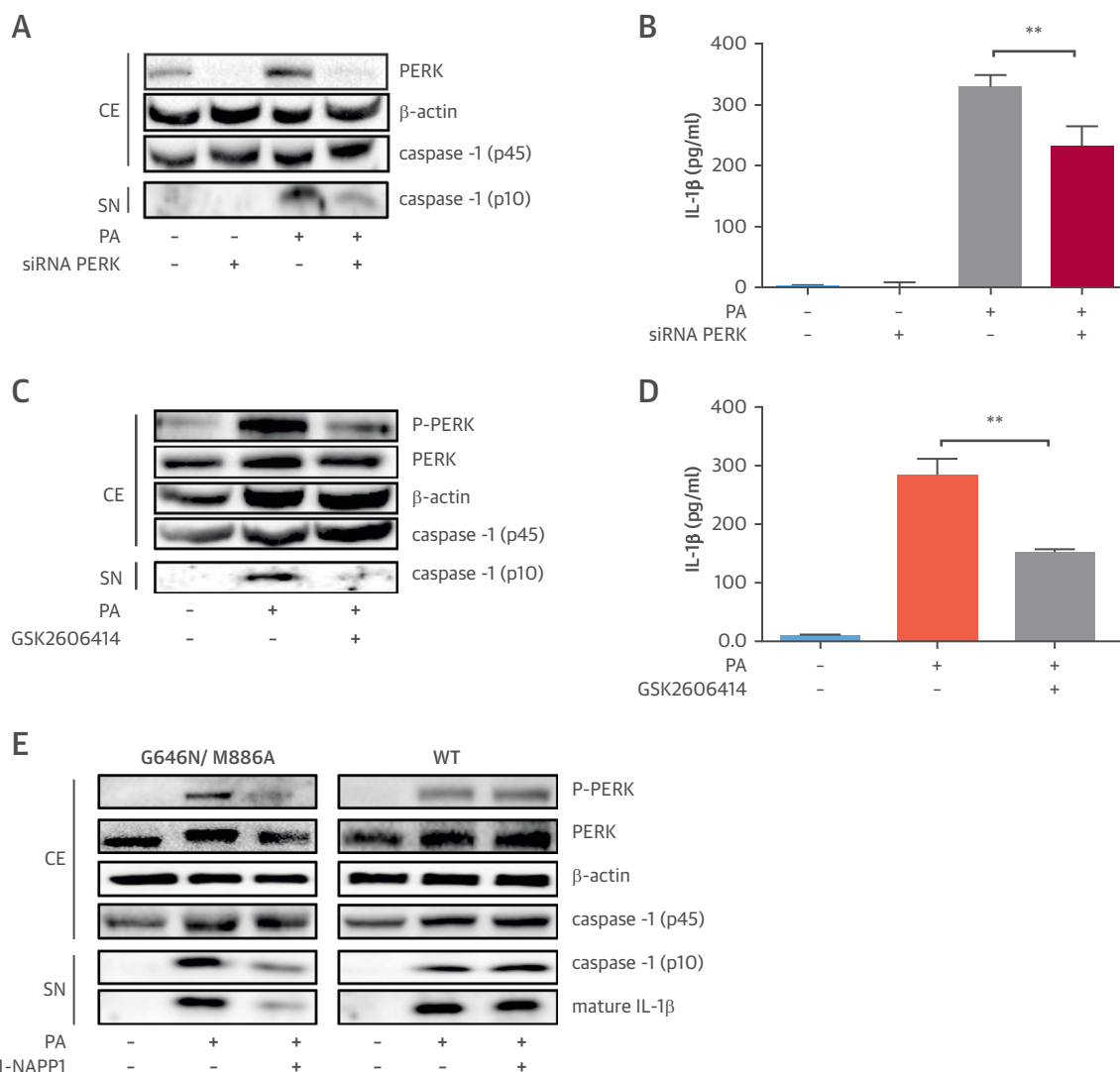
(A and B) LPS-primed, PA-stimulated BMDM were transfected with PERK or control siRNA or **(C and D)** treated with GSK2606414 (2 μmol/l) or vehicle: **(A and C)** protein lysates were analyzed by Western blotting using antibodies against P-PERK, PERK, β-actin, and caspase-1 (p45 and p10), and **(B and D)** conditioned cell medium was analyzed with IL-1β ELISA. **(E)** LPS-primed, PA-stimulated macrophages from PERK_ASKA or WT mice were treated with 1-NAPP1 (20 μmol/l) and protein lysates were analyzed by Western blotting using antibodies against P-PERK, PERK, β-actin, caspase-1 (p45 and p10), and IL-1β. Blots shown are representative of (n = 3) experiments. Data are mean ± SEM; (n = 4) for ELISA. Unpaired *t*-test with Welch's correction. *p ≤ 0.05, **p ≤ 0.01, ***p ≤ 0.001. BMDM = bone marrow-derived macrophages; CE = cell extract; ELISA = enzyme-linked immunosorbent assay; IL = interleukin; LPS = liposaccharide; PA = palmitate; siRNA = silencer RNA; SN = supernatant; WT = wild-type.

treatment of mouse bone marrow-derived macrophages (BMDM) led to profound induction of cleaved caspase-1 (p10 fragment) and IL-1β secretion, but this was significantly reduced by silencer RNA (siRNA)-mediated PERK suppression (**Figures 1A and 1B**, Online Figure 1A). To further assess PERK kinase activity's role in this, lipid-stressed macrophages were treated with a PERK kinase inhibitor (GSK2606414) (21). GSK2606414 suppressed PERK phosphorylation and counteracted lipid-induced caspase-1 cleavage and IL-1β secretion in BMDMs (**Figures 1C and 1D**, Online Figure 1B), human Thp1 macrophages, and human peripheral blood monocytes (PBMC) (Online Figures 1C and 1D). PERK inhibition did not impact the expression of pro-IL-1β, PYD and CARD domain-containing

FIGURE 2 ISR's Critical Role in Lipid-Induced Inflammasome Activation
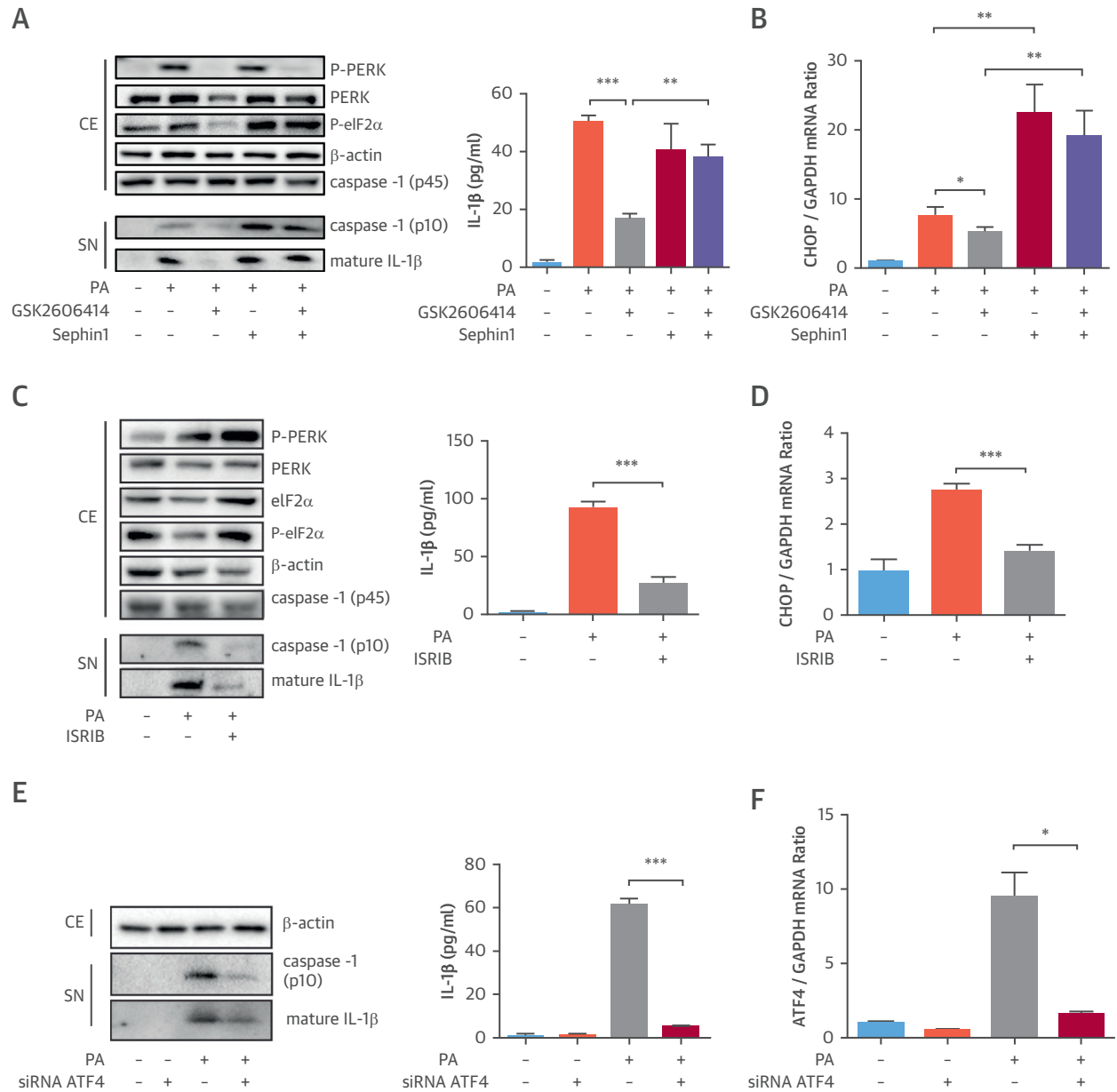
(A and B) LPS-primed, PA-stimulated BMDM were treated with GSK2606414 (2 μmol/l) and/or Sephin1 (25 μmol/l) or **(C and D)** ISRIB (6 μmol/l): **(A and C)** protein lysates were analyzed by Western blotting using antibodies against P-PERK, PERK, P-eIF2α, β-actin, caspase-1 (p45 and p10), and IL-1β, and conditioned cell medium was analyzed with IL-1β ELISA, and **(B and D)** total RNA was analyzed by qRT-PCR for CHOP mRNA. **(E and F)** LPS-primed, PA-stimulated BMDMs were transfected with ATF4 or control siRNAs: **(E)** protein lysates were analyzed by Western blotting using antibodies against: β-actin, caspase-1 (p10), and IL-1β, and conditioned cell medium was analyzed with IL-1β ELISA, and **(F)** total RNA was analyzed by qRT-PCR for ATF4 mRNA. Western blots shown are representative (n = 3) experiments. Data are mean ± SEM; (n = 4) for ELISA and qPCR. Unpaired *t*-test with Welch's correction. *p ≤ 0.05, **p ≤ 0.01, ***p ≤ 0.001. ISR = integrated stress response; qRT-PCR = quantitative reverse transcription polymerase chain reaction; other abbreviations as in **Figure 1**.

protein, and pro-caspase-1 mRNAs, but a small reduction in NLRP3 mRNA was noted (Online Figures 1E and 1F). PERK inhibition also reduced lipid-induced tumor necrosis factor (TNF)-α and C-C motif chemokine ligand-2 (CCL2) mRNA (Online Figures 1E and 1F).

Additionally, we took advantage of the ATP analog sensitive kinase allele (ASKA) of PERK to specifically

modulate PERK's kinase activity (22). The ASKA approach involves a conserved (gatekeeper) amino acid mutation in the deep, hydrophobic ATP-binding kinase pocket, which unblocks access to bulky ATP analogs (23). The M886A mutation on PERK confers the ability to use ATP analogs with bulky alkyl groups (22). To prevent an unstable kinase (24), the PERK_ASKA mice were designed with a second stabilizing mutation at G646N (Online Figures 1G and 1H). 1-NAPP1 selectively suppressed PERK_ASKA kinase activity (along with lipid-induced caspase-1 cleavage and IL-1β secretion in macrophages) but not wild-type PERK's activity (**Figure 1E**, Online Figure 1I), demonstrating PERK kinase activity's role in lipid-induced inflammasome activation.

We next investigated eIF2α's role in lipid-induced inflammasome activation. Sephin1, a small molecule inhibitor of the stress-induced eIF2α regulatory subunit (25,26), lead to persistent eIF2α phosphorylation and CHOP mRNA induction in PERK inhibitor-treated BMDMs (**Figures 2A and 2B,** Online Figure 2A) GSK2606414 inhibited lipid-induced caspase-1 cleavage and IL-1β secretion, but not in Sephin1-treated BMDMs (**Figure 2A,** Online Figure 2A). This finding confirms PERK acts through eIF2α phosphorylation in controlling inflammasome activation.

We next inhibited PERK signaling downstream of eIF2α with a small molecule activator of eIF2B, ISRIB (27). ISRIB did not inhibit lipid-induced PERK activation or eIF2α phosphorylation but blocked stress-induced CHOP mRNA in BMDM and THP-1 macrophages (**Figures 2C and 2D,** Online Figures 1C and 2B). ISRIB led to a profound suppression of lipid-induced caspase-1 cleavage and IL-1β secretion (**Figure 2C,** Online Figures 1C and 2B). ATF4 knockdown also led to marked suppression of PA-induced caspase-1 cleavage and IL-1β secretion (**Figures 2E and 2F,** Online Figure 2C). ISRIB caused a small reduction in lipid-induced NLRP3 mRNA and unexpectedly in pro-IL-1β (Online Figure 2D), but ATF4 knockdown did not impact pro-Il-1β mRNA (Online Figure 2E). Collectively, these findings demonstrate that interrupting ISR signaling can profoundly block lipid-induced inflammasome activation.

PERK-INDUCED MITOCHONDRIAL LON PROTEASE CONTROLS MITOCHONDRIA CLEARANCE AND INFLAMMASOME ACTIVATION. Inflammasome activation by ER stress requires increased mtROS production (18). SFA leads to dramatic elevation of mtROS levels in BMDMs (16), and we observed this is completely blocked by GSK2606414, but not Sephin1 (**Figure 3A,** Online Figures 3A and 3B). ISRIB also suppressed lipid-induced mtROS (**Figure 3A,** Online

Figure 3C), demonstrating ISR's important role in managing mitochondrial oxidative stress.

We next investigated how PERK-eIF2α signaling relays lipid stress to inflammasome activation. ER toxins can up-regulate a mitochondrial matrix, ATP-dependent protease and stress-induced chaperone, LONP1, in a PERK-dependent manner (28,29). PINK1 (a mitochondria localized kinase that phosphorylates Parkinson juvenile disease protein 2 [Parkin] and recruits autophagosomes) is a LONP1 substrate, implicating LONP1 in Parkin-dependent mitophagy (30). Mitophagy counteracts mtROS and inflammasome activation by lipids (16). We asked whether LONP1 plays a role in SFA-induced mtROS production and inflammasome activation. Indeed, PA induced LONP1 expression (**Figure 3B**), which was significantly blocked by GSK2606414 (**Figure 3B**). Sephin1, on the other hand, induced LONP1 and prevented PERK inhibitor's ability to suppress LONP1 (**Figure 3B**). As expected, ISRIB significantly suppressed LONP1 (**Figure 3B**). PERK or ATF4 knockdown also blocked LONP1 induction by lipids (**Figure 3B**). These results demonstrate SFA induces LONP1 through PERK-eIF2α signaling. Furthermore, SFA activates PERK, induces LONP1 (**Figure 3C,** Online Figures 4A to 4D), but reduces PINK1 in macrophages (**Figure 3C,** Online Figure 4A). This inverse regulation is counteracted by GSK2606414 or ISRIB (**Figure 3C,** Online Figures 4A to 4D). To confirm SFA-induced PINK1 reduction was a consequence of LONP1 activation, we silenced LONP1 with siRNA. This led to stabilization of PINK1 levels in lipid-stressed BMDM (**Figure 3D,** Online Figure 4E). These results show SFA leads to PINK1 suppression by activating PERK-eIF2α-LONP1 signaling. Moreover, treatment of lipid-stressed macrophages with GSK2606414 or LONP1 inhibitor (2-cyano-3,12-dioxo-oleana-1,9(11)-dien-28-oic-acid [CDDO]) led to a profound increase in Parkin and autophagy receptor (p62) recruitment to mitochondria (**Figure 3E,** Online Figure 4F). Consistently, expression of a mitochondria import receptor subunit-40 (TOM40) was simultaneously reduced (**Figure 3E,** Online Figure 4F).

We next assessed LONP1's role in mtROS generation. PA induced mtROS in BMDM, but this was significantly blocked by LONP1 knockdown (**Figure 3F,** Online Figure 4G). Suppressing LONP1 also prevented caspase-1 cleavage and IL-1β secretion in lipid-stressed BMDM (**Figures 3G and 3H,** Online Figures 4H and 4I). However, suppressing PINK1 compromised PERK inhibitor's ability to block SFA-induced caspase-1 cleavage and IL-1β secretion (**Figure 3I,** Online Figure 4J). Consistently, GSK2606414, CDDO, or ISRIB could not block SFA-induced IL-1β secretion or caspase-1 cleavage in

**FIGURE 3   PERK-Induced Mitochondrial LON Protease Regulates Mitophagy, mtROS, and Inflammasome Activation**
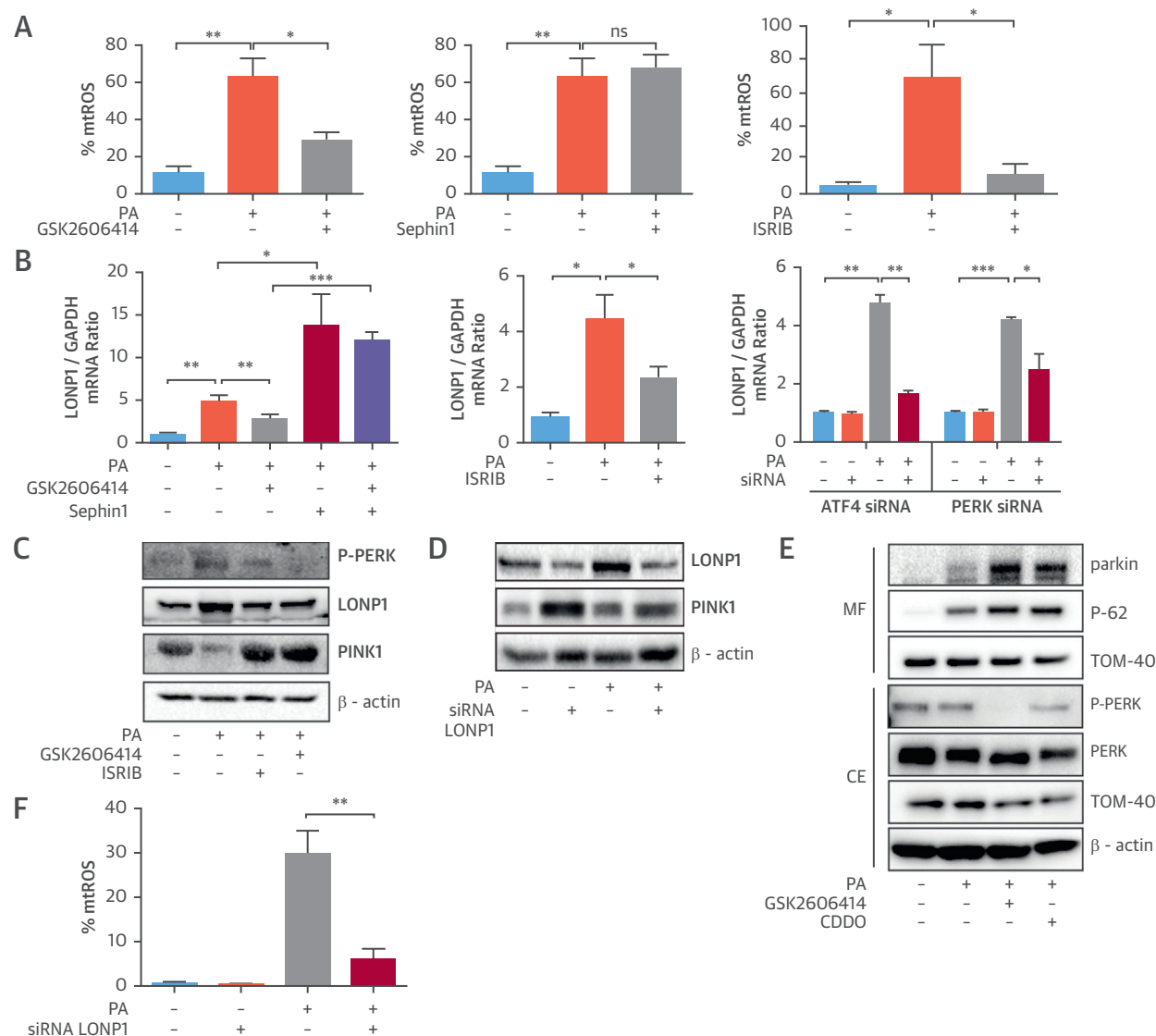
(A to D) LPS-primed, PA-stimulated BMDM were treated with (A) GSK2606414 (2 μmol/l), Sephin1 (25 μmol/l) or ISRIB (6 μmol/l) and mtROS was measured with MitoSOX Red mitochondrial superoxide indicator, or (B) treated with GSK2606414 (2 μmol/l), Sephin1 (25 μmol/l), or ISRIB (6 μmol/l) or transfected with PERK or ATF4 siRNA and total RNA was analyzed by qRT-PCR for LONP1 and GAPDH mRNA, or (C) treated with GSK2606414 (2 μmol/l) or ISRIB (6 μmol/l) and protein lysates were analyzed by Western blotting using antibodies against P-PERK, LONP1, PINK1, and β-actin, or (D) transfected with a LONP1 siRNA and protein lysates were analyzed by Western blotting using antibodies against LONP1, PINK1 and β-actin. (E) Mitochondrial fraction protein lysates from PA-treated RAW264.7 macrophages were analyzed by Western blotting with antibodies against Parkin, p-62, TOM-40, whereas total cell protein extracts were analyzed using antibodies against P-PERK, PERK, TOM-40, and β-actin. (F–H) LPS-primed, PA-stimulated BMDM were (F) transfected with LONP1 siRNA, and mtROS was measured with MitoSOX kit, or (G) transfected with LONP1 siRNA and supernatants were analyzed with IL-1β ELISA, whereas protein lysates were analyzed by Western blotting using antibodies against caspase-1 (p45 and p10), β-actin, and IL-1β, and total RNA was analyzed by qRT-PCR for LONP1 and GAPDH mRNA, or (H) treated with 1 μmol/l CDDO and supernatants were analyzed with IL-1β ELISA, whereas protein lysates were analyzed by Western blotting using antibodies against caspase-1 (p45 and p10), β-actin, and IL-1β, or (I) transfected with PINK1 siRNA and/or treated with GSK2606414 (2 μmol/l); the conditioned medium was analyzed by IL-1β ELISA or Western blotting using antibodies against caspase-1 (p10) and IL-1β, whereas total RNA was analyzed by qRT-PCR for PINK1 and GAPDH mRNA. (J) LPS-primed *Parkin*^{−/−} or WT BMDM were treated with PA and GSK2606414 (2 μmol/l) or CDDO (1 to 2 μmol/l); conditioned cell medium was analyzed with IL-1β ELISA or by Western blotting using antibodies against caspase-1 (p45 and p10), β-actin, and IL-1β. Western blots shown are representative. Data are mean ± SEM; (n = 3) for Western blots and (n = 4) for ELISA and qPCR. Unpaired *t*-test with Welch's correction. *p ≤ 0.05, **p ≤ 0.01, ***p ≤ 0.001. mtROS = mitochondrial reactive oxygen species; ns = not significant; other abbreviations as in **Figures 1 and 2**.
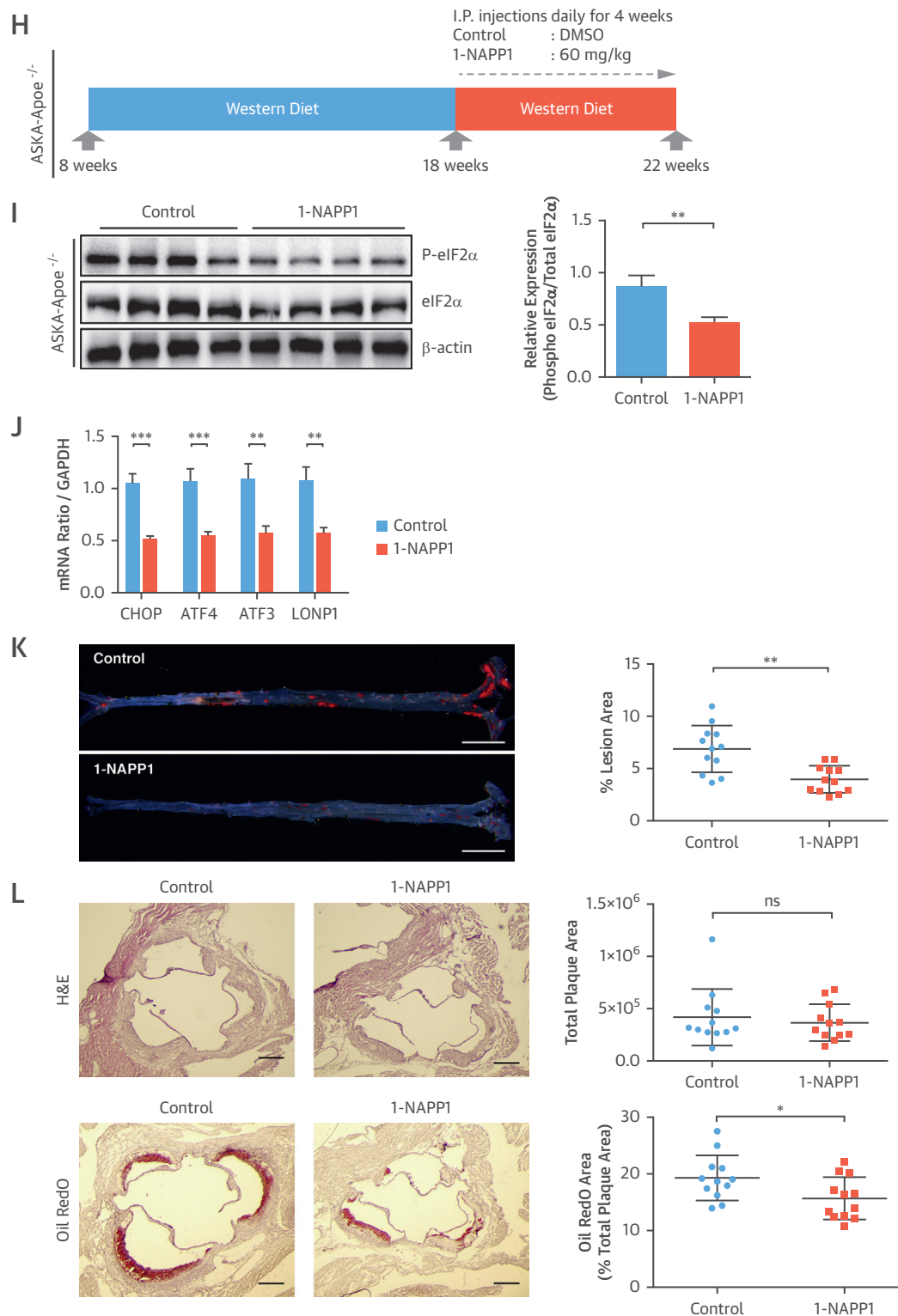
FIGURE 3 Continued
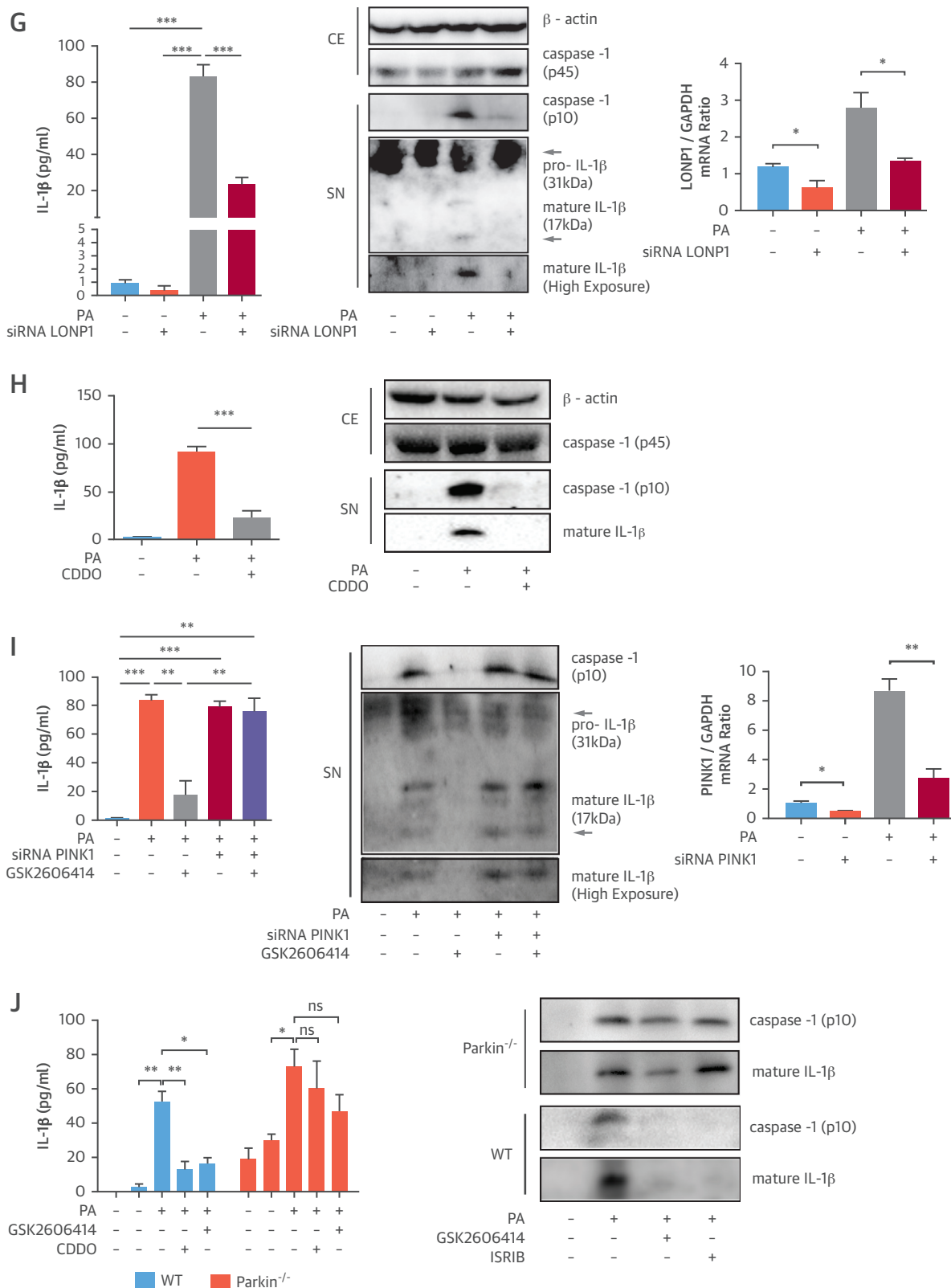
FIGURE 4 PERK Inhibition Leads to Reduction in Plaque Area in *Apoe*$^{-/-}$ Mice
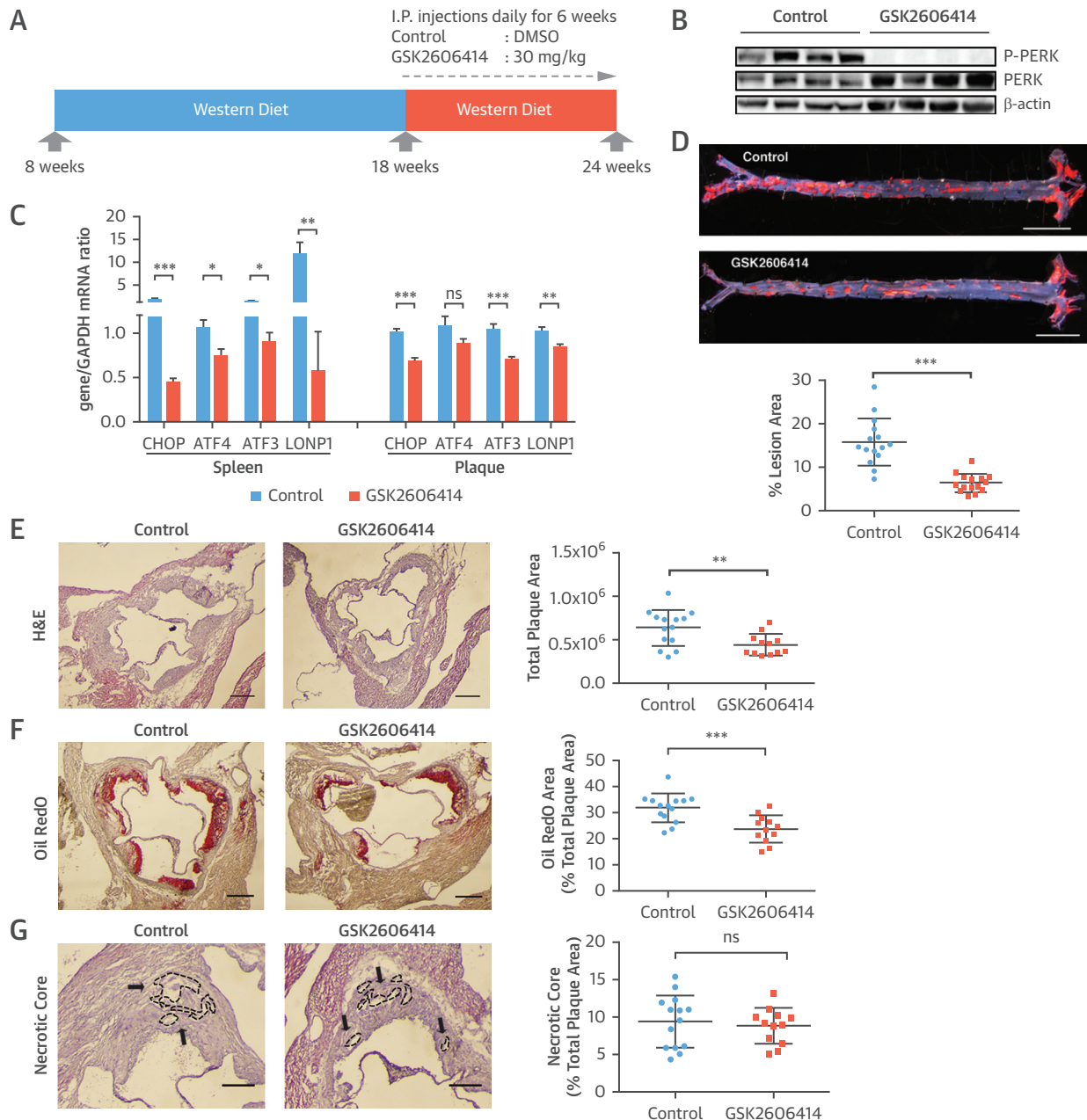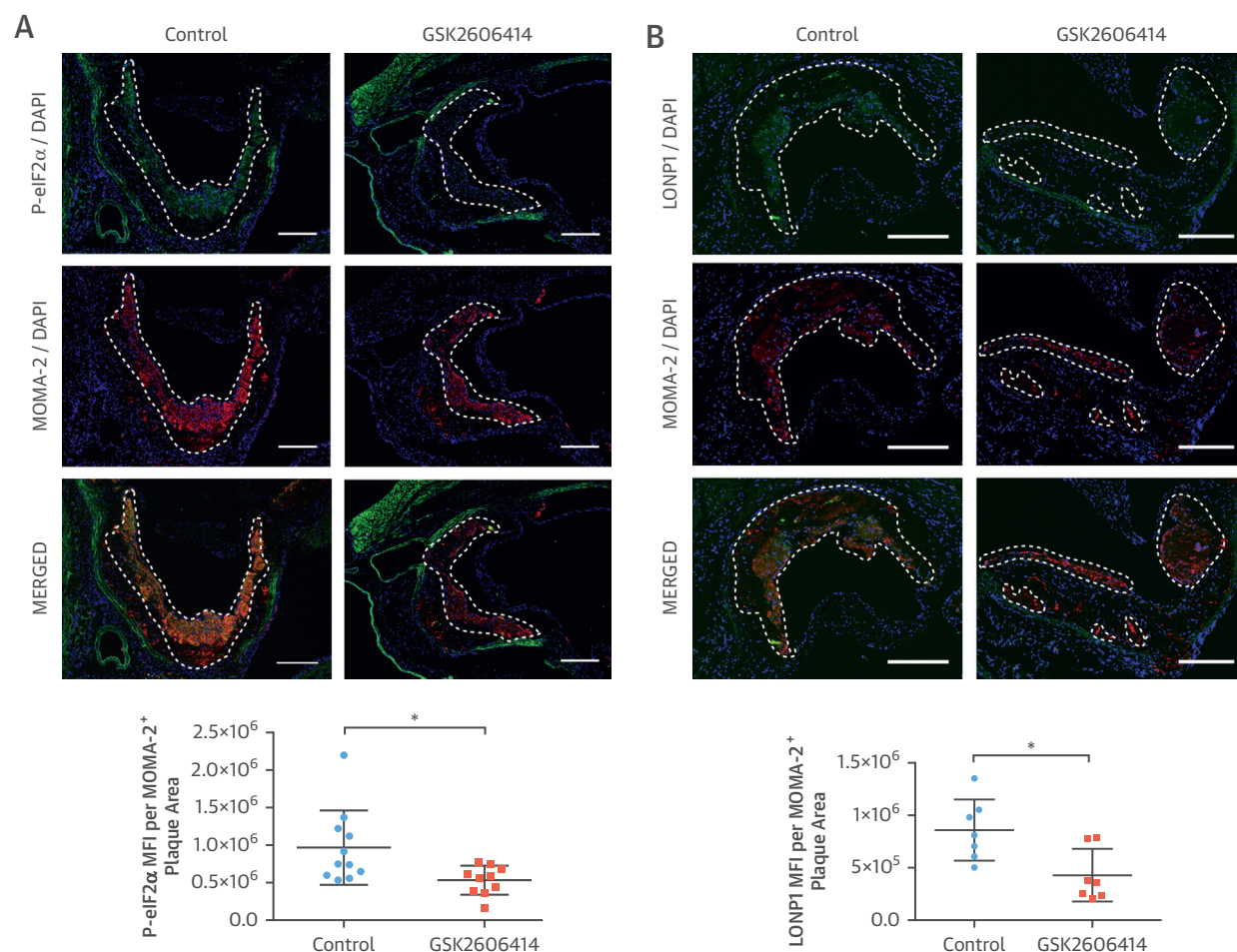

(A to G) Experimental design in *Apoe*$^{-/-}$ mice treated with a PERK inhibitor: **(A)** GSK2606414 (30 mg/kg/day) or vehicle (DMSO). **(B)** Pancreas protein lysates were analyzed by Western blotting using antibodies against P-PERK, PERK, and β-actin (n = 4 control group, 4 treatment group). **(C)** Spleen **(left)** or aortic root plaques **(right)** total RNA were analyzed by qRT-PCR for CHOP, ATF4, ATF3, and LONP1 mRNA (n = 14 control group, 12 treatment group). **(D)** Lesion area was calculated from en face aorta preparations stained with Sudan IV (n = 15 control group, 15 treatment group; scale bar: 5 mm). **(E)** Total plaque area was calculated from H&E-stained (n = 14 control group, 12 treatment group), **(F)** foam cell area was calculated from Oil RedO-stained (n = 14 control group, 12 treatment group), whereas **(G)** necrotic area was calculated from H&E-stained aortic root sections (n = 14 control group, 12 treatment group) (scale bar: 300 μm). **(H)** Experimental design in PERK_ASKA, *Apoe*$^{-/-}$ mice treated with 1-NAPP1 (60 mg/kg/day) or vehicle in the control mice: **(I)** Pancreas protein lysates were analyzed by Western blotting using antibodies against P-eIF2α, eIF2α, and β-actin (bands quantification and displayed next to blot; n = 4 control group, 4 treatment group). **(J)** Aortic root plaque total RNA was analyzed by qRT-PCR for CHOP, ATF4, ATF3, and LONP1 mRNA (n = 10 control group, 10 treatment group). **(K)** Lesion area was calculated from Sudan IV-stained en face aorta preparations (n = 12 control group, 12 treatment group) (scale bar: 5 mm) and **(L)** total plaque area from H&E-stained aortic root sections **(upper panel)**, whereas foam cell area was calculated from Oil RedO-stained sections **(lower panel)** (n = 12 control group, 12 treatment group) (scale bar: 300 μm). Data are mean ± SEM. Mann-Whitney *U* test. *p ≤ 0.05, **p ≤ 0.01, ***p ≤ 0.001. DMSO = dimethyl sulfoxide; H&E = hematoxylin and eosin; other abbreviations as in **Figures 1, 2, and 3**.

FIGURE 4   Continued

H

ASKA-Apoe⁻/⁻

I.P. injections daily for 4 weeks
Control   : DMSO
1-NAPP1   : 60 mg/kg

Western Diet   Western Diet

8 weeks   18 weeks   22 weeks

I

ASKA-Apoe⁻/⁻

Control   1-NAPP1

P-eIF2α
eIF2α
β-actin

J

K

Control
1-NAPP1

L

Control   1-NAPP1
H&E

Control   1-NAPP1
Oil RedO

FIGURE 5   PERK Inhibitor Suppresses Hyperlipidemia-İnduced Inflammation in *Apoe*⁻/⁻

(A–G) Immunohistochemical analysis of aortic root cryosections from GSK2606414- or vehicle (DMSO)-treated *Apoe*⁻/⁻ (mice as in **Figure 4**). A representative image is shown for the quantification: **(A and B)** MFI **(green)** quantified from macrophage positive area **(red) (A)** P-eIF2α (n = 11 control group, 10 treatment group), **(B)** LONP1 (n = 7 control group, 7 treatment group), **(C)** MOMA-2 (n = 11 control group, 10 treatment group), **(D)** CD3 (n = 12 control group, 10 treatment group), **(E)** α-SMA (n = 14 control group, 12 treatment group), and **(F)** Masson's Trichrome (n = 11 control group, 10 treatment group), **(G)** IL-1β (MFI) **(green)** quantified from the macrophage area **(red)** (n = 11 control group, 10 treatment group). **(H)** Aortic root plaque RNA was analyzed by qRT-PCR for pro-IL-1β expression (n = 14 control group, 12 treatment group). **(I)** Immunohistochemical analysis of aortic root cryosections for caspase-1 (FAM-FLICA, **green**), from MOMA-2-positive **(red)** area (n = 7 control group, 8 treatment group). **(J)** Plasma IL-18 (**left**; n = 8 control group, 8 treatment group) or IFNγ (**right**; n = 7 control group, 7 treatment group) were measured with ELISA. Data are mean ± SEM; Mann-Whitney *U* test. *p ≤ 0.05, **p ≤ 0.01, ***p ≤ 0.001. (Scale bar: 200 μm except in **D**: 50 μm). MFI = mean fluorescent intensity; other abbreviations as in **Figures 1, 2, 3, and 4.**

Parkin-deficient BMDMs (**Figure 3J**, Online Figure 4K). These collective results demonstrate ISR inhibits PINK1-Parkin-dependent mitophagy, elevates mtROS, and activates the inflammasome in lipid-stressed macrophages.

INHIBITION OF PERK KINASE MITIGATES ATHEROSCLEROSIS. Organelle stress drives atherosclerosis progression (14,31). We next assessed whether inhibiting PERK could prevent atherosclerosis progression (32). To test this, we challenged

Apoe⁻/⁻ mice with the Western diet (16 weeks) and injected GSK2606414 (30 mg/kg/day) (6 weeks) (**Figure 4A**) (33). No significant differences in plasma glucose and insulin levels or blood cell counts were observed between the groups (Online Figures 5A and 5B). We confirmed the inhibitor engaged its molecular target effectively by assessing PERK autophosphorylation and CHOP and ATF3 mRNA (**Figures 4B and 4C**, Online Figure 5C). We detected no improvement in plasma lipids or lipoproteins

FIGURE 5 Continued
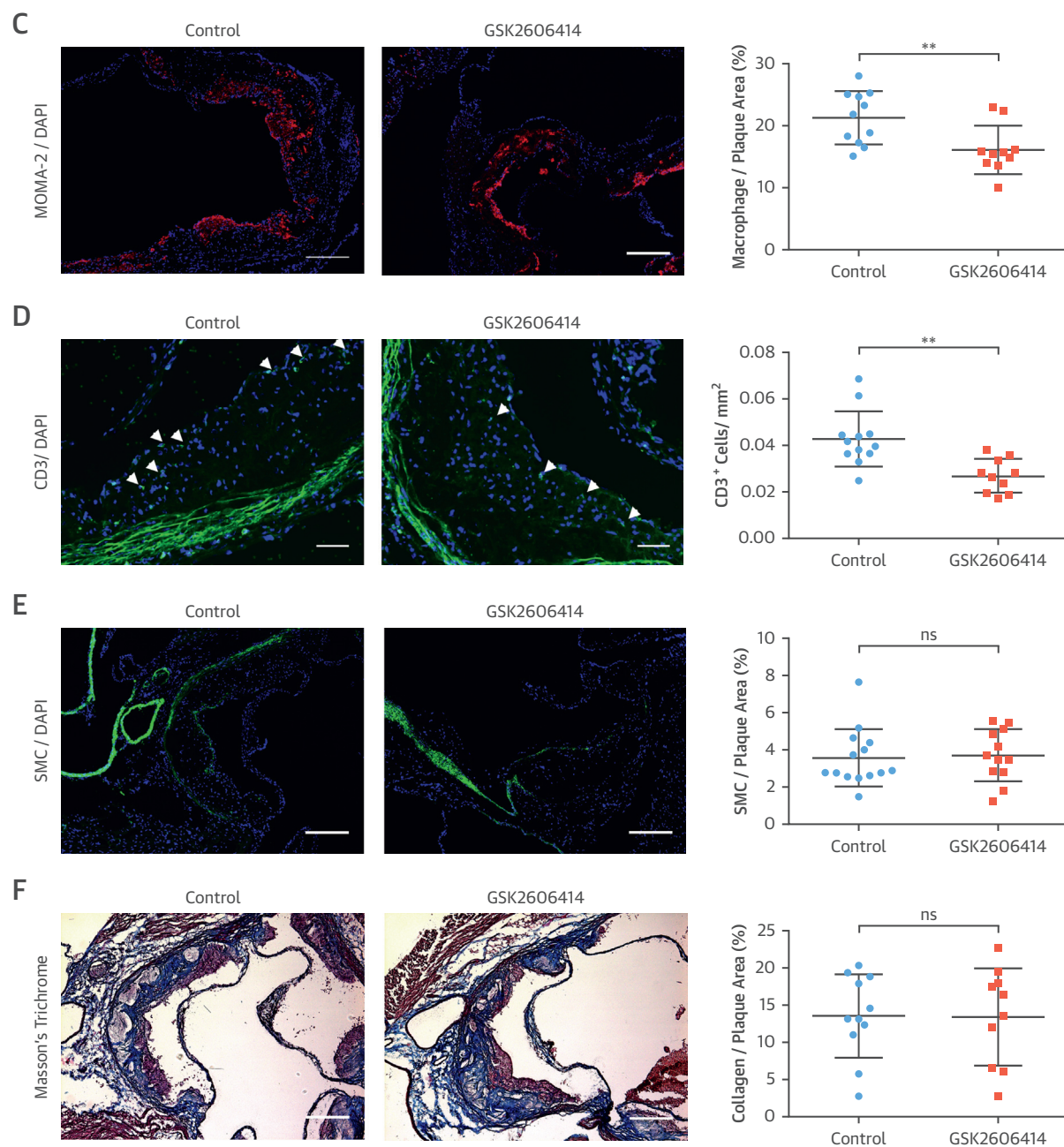
Continued on the next page

(Online Figures 5D-5G); however, GSK2606414 led to a significant decrease in atherosclerotic lesions in en face aorta preparations (44%) (**Figure 4D**, Online Figure 6A). GSK2606414 significantly reduced aortic root plaque (32%) (**Figure 4E**) and foam cell area (25%) (**Figure 4F**, Online Figure 6B). No significant changes in the plaque necrotic area or apoptotic cell numbers were noted between the groups (**Figure 4G**,

Online Figure 6C). There was a reduction in plaque VCAM-1 protein (33%) (Online Figure 6D), and CCL2 (20%) (Online Figure 6E), and serum monocyte chemoattractant protein-1 (46%) (Online Figure 6F) after PERK inhibition, suggesting macrophage recruitment is impacted.

We also analyzed atherosclerosis in the PERK_ASKA, $Apoe^{-/-}$ transgenic mice. These mice
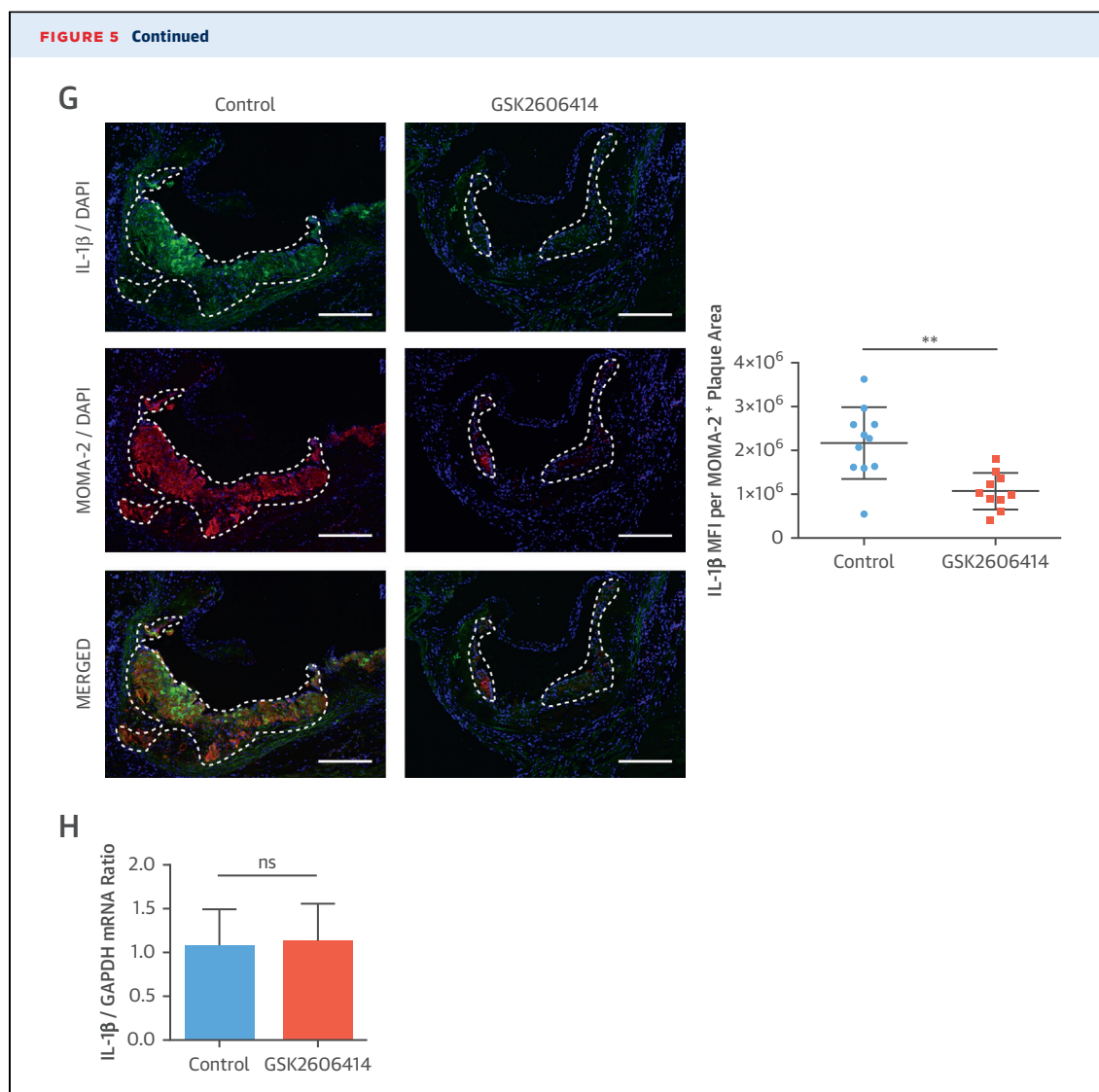
FIGURE 5 Continued

Continued on the next page

were fed the Western diet (14 weeks) and treated with 1-NAPP1 (60 mg/kg/day, 4 weeks) (**Figure 4H**). 1-NAPP1 inhibited eIF2α phosphorylation (**Figure 4I**) and CHOP, ATF4, and ATF3 mRNA (**Figure 4J**). Although there were no significant differences in systemic metabolic parameters between the groups (Online Figures 7A and 7B), 1-NAPP1 significantly reduced atherosclerotic lesions in en face aorta preparations (45%) (**Figure 4K**) and aortic root foam cell area (20%), but not plaque area (**Figure 4L**). These findings in the PERK_ASKA mouse model confirm the atheroprotection we observed in mice treated with the PERK inhibitor.

PERK INHIBITION BLOCKS HYPERLIPIDEMIA-INDUCED INFLAMMATION IN VIVO. Macrophages and other immune cells infiltrate plaques during atherogenesis

(34). We next analyzed the impact of PERK inhibition on plaque cellular composition. GSK2606414 and 1-NAPP1 both lead to significant reduction in P-eIF2α in plaque macrophage-rich areas (GSK2606414: 45%) (**Figure 5A**), (1-NAPP1: 50%) (Online Figure 7C), as well as CHOP and ATF3 mRNA (GSK2606414: both 33%) (**Figure 4C**), (1-NAPP1: CHOP 50%; ATF3: 48%) (**Figure 4J**). PERK inhibition reduced LONP1 (GSK2606414: 49%) (**Figure 5B**), (GSK2606414: 20%) (**Figure 4C**), and (1-NAPP1: 48%) (**Figure 4J**). Fewer macrophages (GSK2606414: 25%) (**Figure 5C**) (1-NAPP1: 33%) (Online Figure 7D) and T cells (GSK2606414: 45%) (**Figure 5D**) were observed in plaques, but vascular smooth muscle cells and collagen content were not altered by GSK2606414 (**Figures 5E and 5F**). On the basis of these results, the

FIGURE 5   Continued
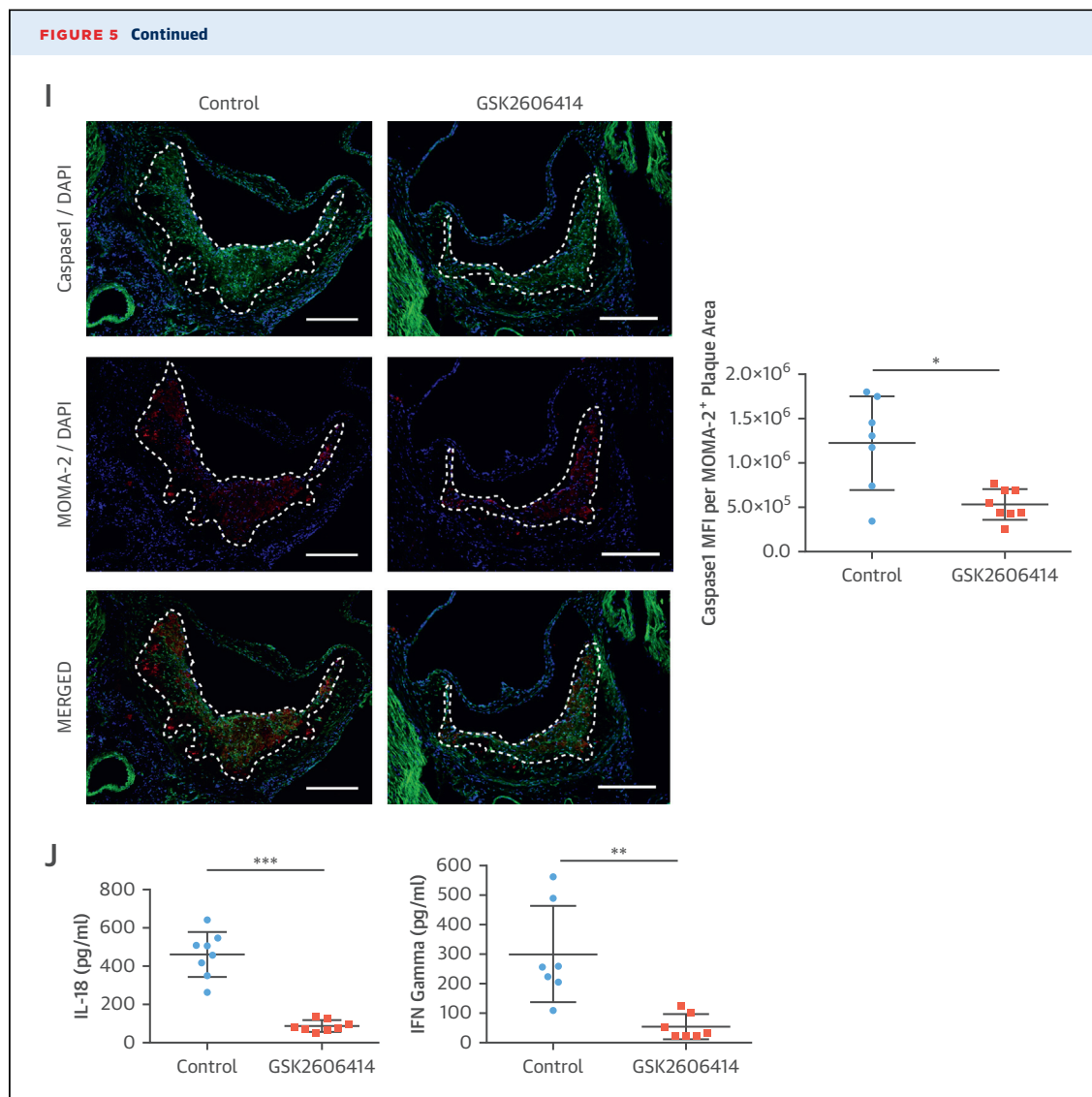
major consequence of PERK inhibition on plaques is reduced immune cells and lipid content.

PERK inhibition led to a significant inhibition of hyperlipidemia-induced expression of plaque IL-1β protein (GSK2606414: 45%) (**Figure 5G**), (1-NAPP1: 47%) (Online Figure 7E), but not IL-1β mRNA (**Figure 5H,** Online Figure 7F). However, PERK inhibition reduced CCL2 and TNFα mRNA levels in plaques (GSK2606414: 20% and 30%, respectively) (Online Figure 6E) (1-NAPP1: 48% and 47%, respectively) (Online Figure 7G). PERK inhibition reduced active caspase-1 (both 50%) (GSK2606414: **Figure 5I,** 1-NAPP1: Online Figure 7H). Consistently, PERK inhibitor reduced IL-18 (80%) (**Figure 5J**) and IFNγ (80%) (**Figure 5J**).

BLOCKING THE ISR WITH ISRIB COUNTERACTS ATHEROSCLEROSIS. We next investigated the

consequences of modulating eIF2B for atherosclerosis in vivo. *Apoe*$^{-/-}$ mice on the Western diet (15 to 16 weeks) were injected with ISRIB (1 mg/kg/day; 6 weeks, 2 mg/kg/day; 5 weeks) (**Figure 6A**) (35). ISRIB did not inhibit eIF2α phosphorylation in vivo but reduced CHOP, ATF3, and LONP1 mRNAs (**Figures 6B and 6C**). There were no significant differences in metabolic parameters or blood cell counts between the groups (Online Figures 8A to 8D), but ISRIB caused a significant decrease in lesions in en face aorta preparations (1 mg/kg 26% and 2 mg/kg 39%) (**Figure 6D,** Online Figure 8E). ISRIB did not alter plaque area (**Figure 6E**) but reduced aortic root foam cell area (1 mg/kg 28%, 2 mg/kg 32%) (**Figure 6F,** Online Figure 8F). ISRIB also did not alter plaque necrotic area (**Figure 6G**).

FIGURE 6   Blocking ISR by ISRIB Alleviates Atherosclerosis
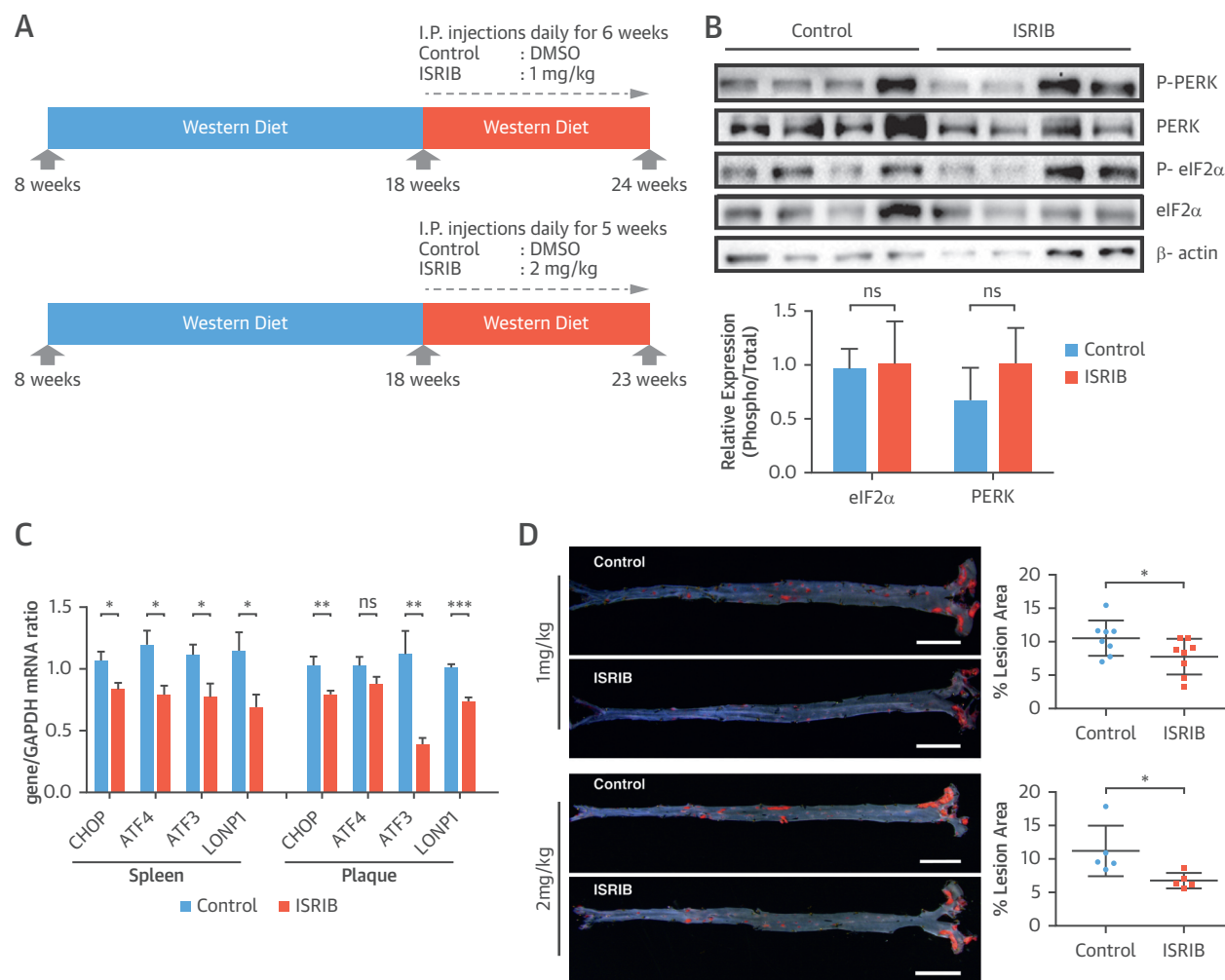
(A) Experimental design in *Apoe*$^{-/-}$ mice treated with ISRIB (1 to 2 mg/kg/day) or vehicle. (B) Pancreas protein lysates were analyzed by Western blotting with antibodies against P-PERK, PERK, P-eIF2α, eIF2α, and β-actin (n = 4 control group, 4 treatment group) (quantification of bands are below the blot); and (C) spleen (left) or aortic root plaque (right) total RNA was analyzed by qRT-PCR for CHOP, ATF4, ATF3, and LONP1 expression (n = 7 control group, 8 treatment group). (D) Lesion area was calculated from Sudan IV–stained en face aorta preparations (1 mg/kg ISRIB; n = 8 control group, 8 treatment group; 2 mg/kg ISRIB; n = 5 control group, 5 treatment group) (scale bar: 5 mm). (E) Total plaque area was calculated from H&E-stained and (F) foam cell area from Oil RedO-stained aortic root lesions, whereas (G) necrotic area was calculated from H&E-stained aortic root sections (1 mg/kg; n = 7 control group, 8 treatment group; 2 mg/kg ISRIB; n = 4 control group, 5 treatment group) (scale bar: 300 μm). Data are mean ± SEM. Mann-Whitney *U* test. *p ≤ 0.05. Abbreviation as in Figures 1, 2, 4, and 5.

ISRIB significantly reduced LONP1 expression in macrophage-rich plaque areas (protein: 35%) (Figure 7A) (mRNA: 30%) (Figure 6C). ISRIB significantly reduced plaque macrophages and T cells (23% and 45%, respectively) (Figures 7B and 7C), IL-1β protein (38%) (Figure 7D), but not IL-1β mRNA (Figure 7E), and reduced active caspase-1 (50%) (Figure 7F). Consistently, ISRIB reduced systemic IL-18 levels (45%) (Figure 7G) and plaque CCL2 and TNFα mRNA (59% and 58%, respectively) (Figure 7H). These collective results demonstrate ISR suppression by ISRIB can mitigate lipid-induced inflammation and plaque development.
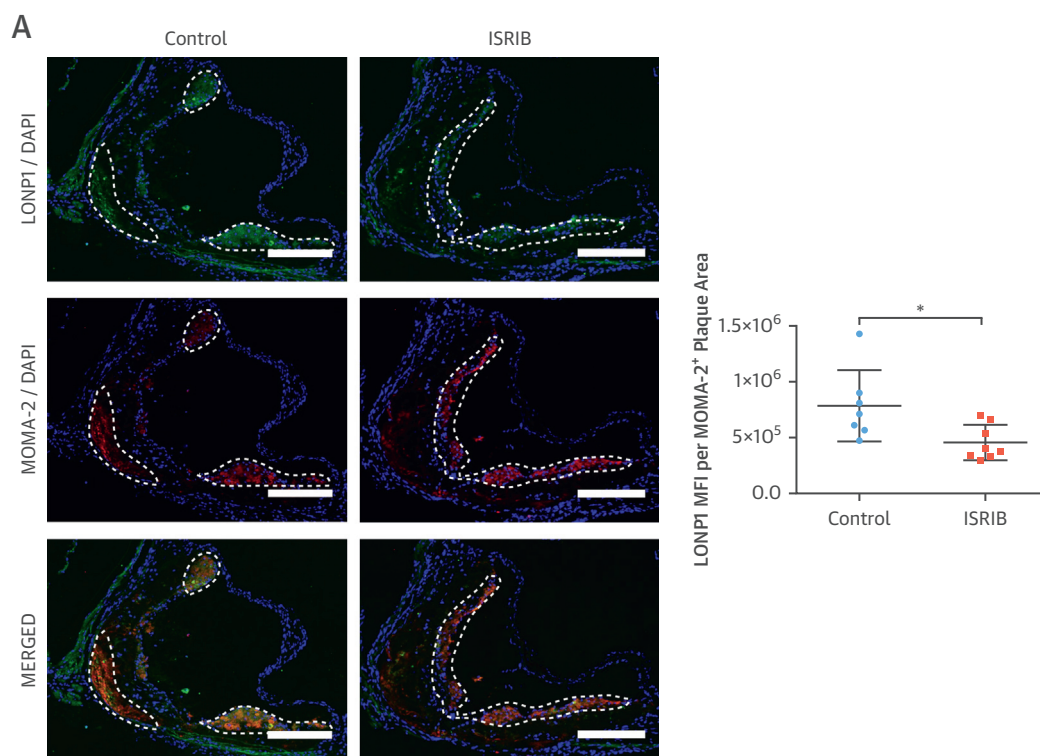
DISCUSSION

Persistent PERK activation and eIF2α phosphorylation is observed in atherosclerotic plaques (5,8). The targetability of ISR was recently assessed in neurodegenerative diseases, identifying potent and specific

FIGURE 6   Continued
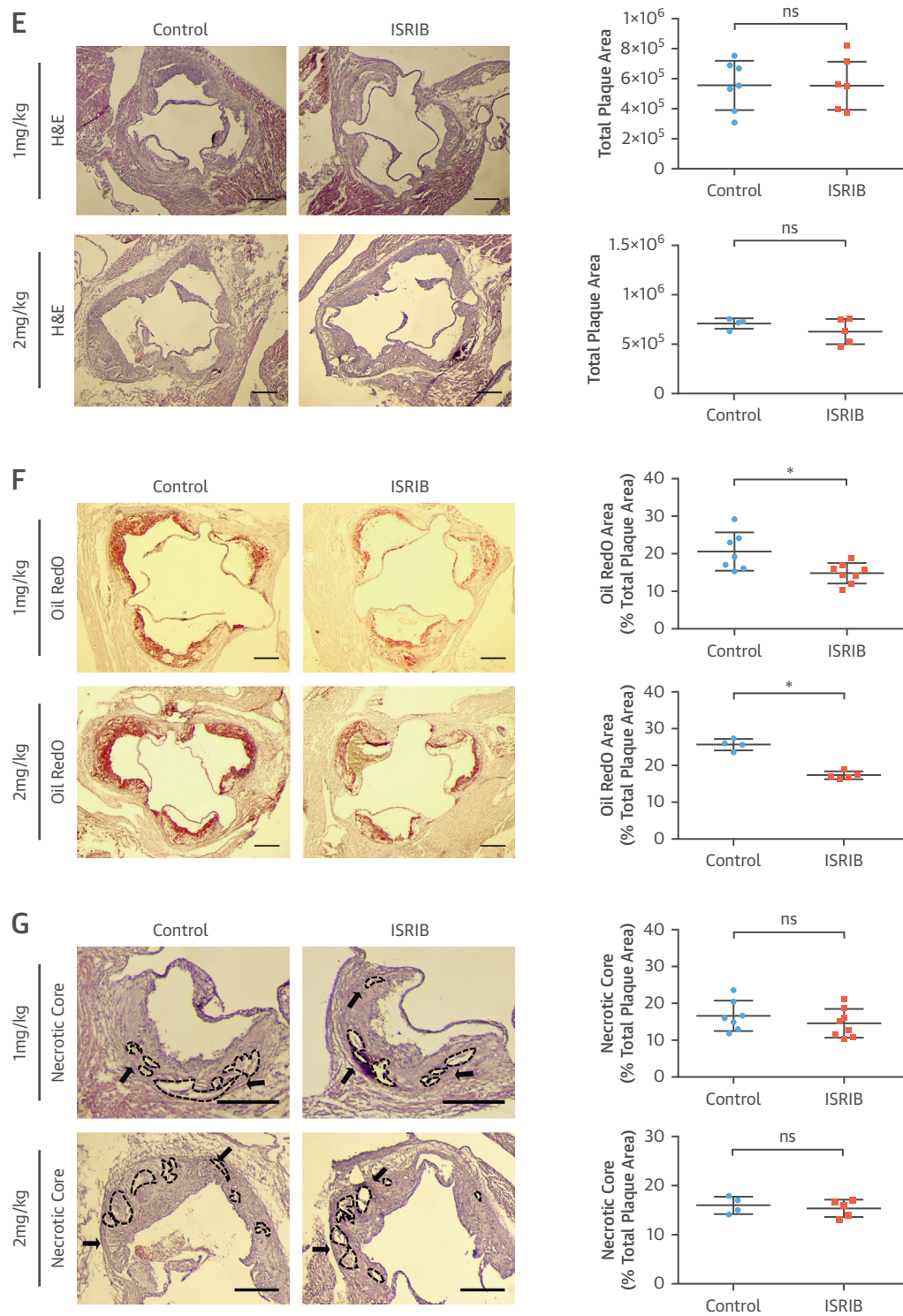
FIGURE 7   ISRIB Suppressed Hyperlipidemia-Induced LONP1 and Inflammation in *Apoe*$^{-/-}$

(A–D) Immunohistochemical analysis of aortic root cryosections (1 mg/kg/day ISRIB-injected mice, as in **Figure 6**); a representative image **(left)** is shown for the quantification: **(A)** LONP1 (MFI) **(green)** quantified from macrophage-positive area **(red)**, **(B)** MOMA-2, **(C)** CD3, and **(D)** IL-1β (MFI) **(green)** quantified from macrophage-positive area **(red)** (n = 7 control group, 8 treatment group). **(E and F)** Total aortic root plaque RNA was analyzed by qRT-PCR for **(E)** IL-1β, and **(F)** CCL2 and TNFα mRNAs (n = 7 control group, 8 treatment group). **(G)** Immunohistochemical analysis of aortic root cryosections for Caspase1 MFI (FAM-FLICA, **green**) quantified from macrophage-positive area **(red)** (n = 7 control group, 8 treatment group). **(H)** Plasma IL-18 levels was measured with ELISA (from mice as shown in **Figure 6**) (n = 8 control group, 8 treatment group). Data are mean ± SEM; Mann-Whitney *U* Test.*p ≤ 0.05, **p ≤ 0.01, ***p ≤ 0.001. (Scale bar: 200 μm; except **C**: 50 μm). Abbreviation as in **Figures 1, 2, 3, and 5**.

small molecule modulators (25-27,35-39). Using these powerful chemical tools, we investigated ISR's role in lipid-induced inflammation and atherosclerosis. To alleviate concerns with possible off-target effects, we utilized multiple drugs that target 3 different molecular players in ISR (39,40). Complementary approaches such as PERK_ASKA mutant or knockdown of key players in the ISR pathway confirmed our main mechanistic finding that PERK-eIF2α-LONP1 pathway couples the stress responses of ER and mitochondria and potentiates inflammasome activation and inflammation induced by dietary fats, thus promotes atherosclerosis.

ISR's ROLE IN INTERORGANELLE COMMUNICATION AND STERILE INFLAMMATION. LONP1 is an important mitochondrial target that is regulated by lipid-induced PERK-eIF2α signaling in macrophages

and in lesions. We discovered that LONP1 plays an unprecedented role during prolonged ER stress by limiting mitochondrial clearance through degrading PINK1. Chronic ER stress caused by dietary fats and activation of PERK-eIF2α-LONP1 signaling can therefore sustain high mtROS levels that flame the inflammasome and drive inflammatory cytokine production during atherogenesis (**Central Illustration**). These findings demonstrate ISR's role in sterile inflammation by modulating organelle stress responses that are important for inflammasome activation by lipids. We observed ISR inhibition suppresses TNFα and CCL2 mRNA induction by lipids, and this may be in part due to the suppression of IL-1β and IL-18 cytokine signaling or ISR's known inhibitory effect on inflammatory transcription factors. Furthermore, yet uncharacterized mitochondria-
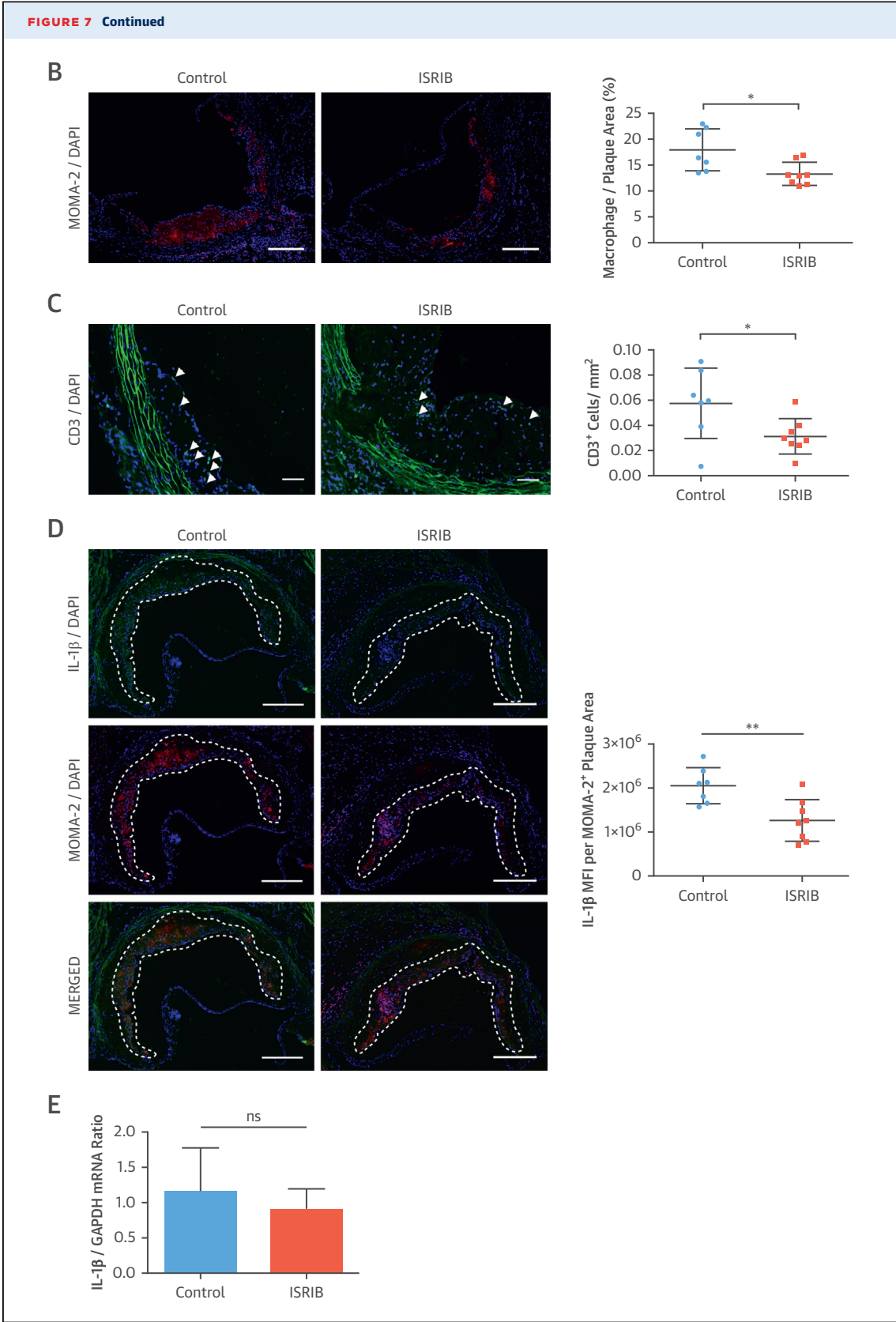
FIGURE 7 Continued

FIGURE 7   Continued
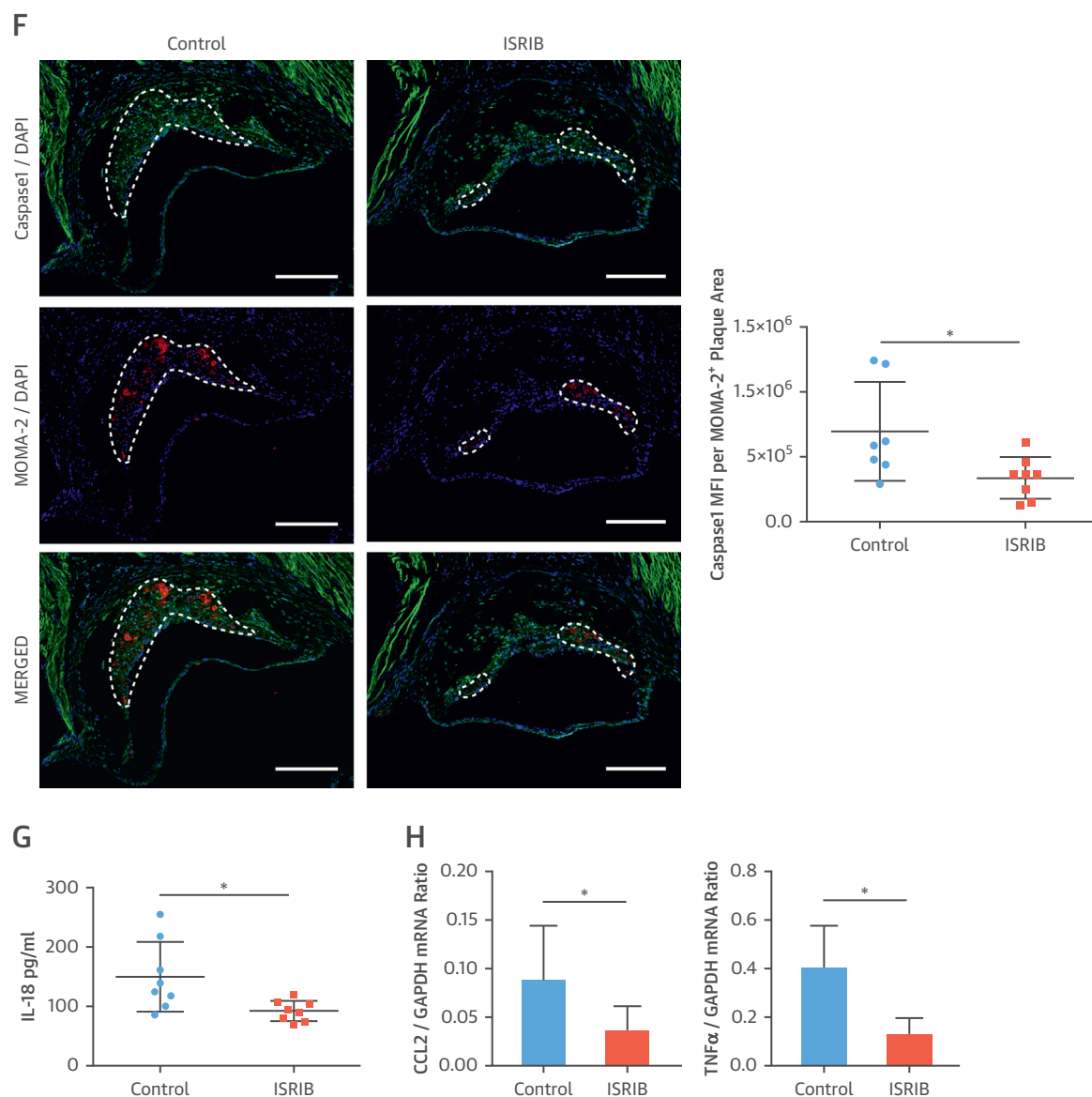
driven metabolic shifts driven by ISR inhibitors could alter the immune epigenome. Our results also suggest LONP1 drives sterile inflammation and atherosclerosis, but this possibility needs to be directly tested. These findings underscore the intricate exchange of information between ER and mitochondria is important for metabolic health and its disruption by dietary fats can promote inflammation and atherosclerosis.

ORGANELLE THERAPEUTICS AS AN UPSTREAM MODULATOR OF IL-1β.

Lipid-induced NLRP3 activation in plaque macrophages is an important contributor to atherosclerosis. Previous studies showed

inflammasome inhibition or antagonizing IL-1β or IL-18 can reduce atherosclerosis independent of an improvement in dyslipidemia (41-43). Furthermore, the results of the CANTOS (Cardiovascular Risk Reduction Study [Reduction in Recurrent Major CV Disease Events]) (neutralizing IL-1β) showed a modest, but significantly lower, rate of recurrent cardiovascular events in patients with previous myocardial infarction, supporting the inflammatory basis of atherothrombosis in humans (44,45). On the other hand, emerging data suggest that IL-1β inhibition can significantly increase the risk of infections (Group A *Streptococcus* [GAS] [46] and Food and Drug

CENTRAL ILLUSTRATION Modulation of the Integrated Stress Response in Atherosclerosis
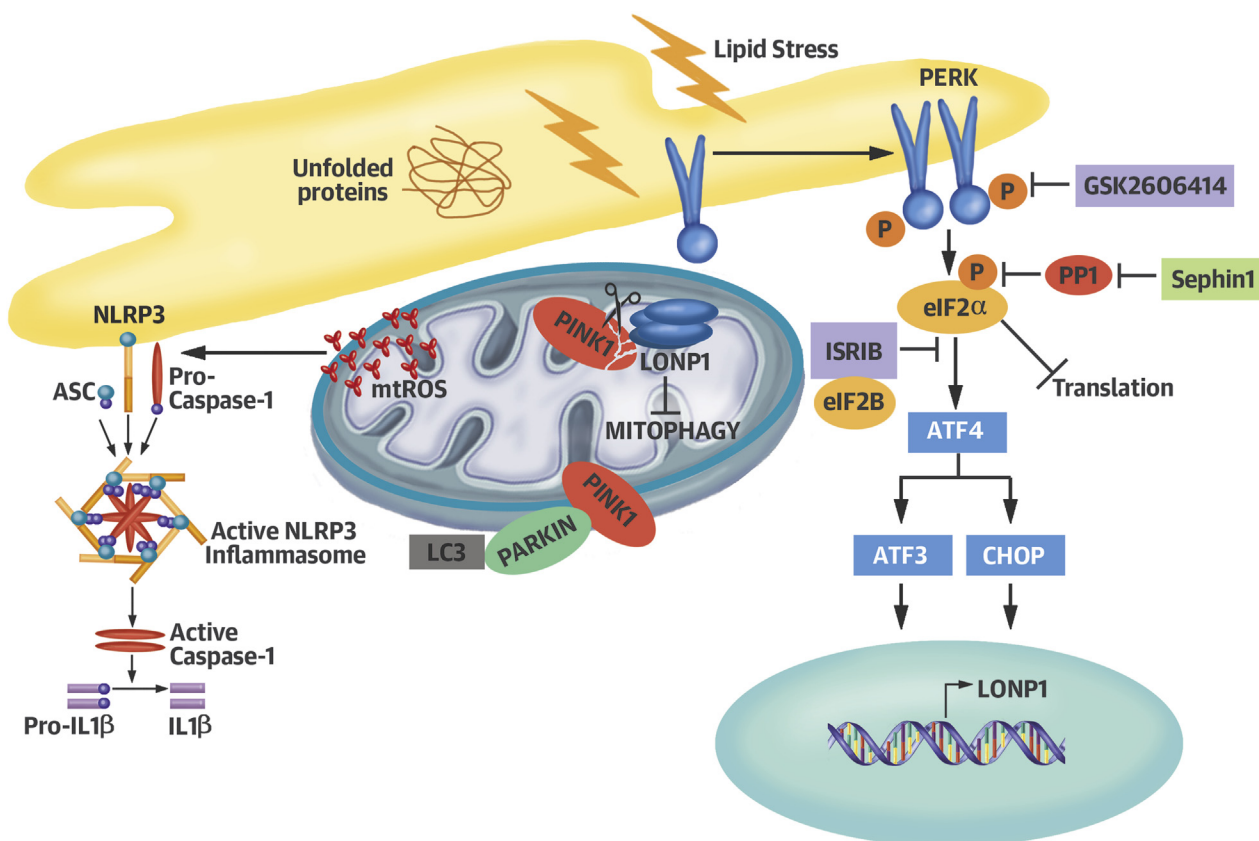
Onat, U.I. et al. J Am Coll Cardiol. 2019;73(10):1149–69.

The integrated stress response (ISR) controls mitochondrial clearance, mtROS production, and NLRP3 inflammasome activation by lipids. Lipid-induced PERK-eIF2α signaling activates a mitochondrial target, LONP1, which degrades its substrate PINK1 and suppresses Parkin-dependent mitophagy. Inhibition of PERK-eIF2α-LONP1 signaling by small molecules promotes mitophagy and counteracts NLRP3 inflammasome by lipids. mtROS = mitochondrial reactive oxygen species.

Administration Adverse Event Reporting System). IL-1 receptor (R)-deficient mice (47) as well as anakinra (IL-1R antagonist)-treated mice display impaired bacterial killing, hypersusceptibility to GAS infection/ dissemination (46). However, caspase-1-deficient, NLRP3-deficient mice or NLRP3 inhibitor–treated mice do not display increased GAS susceptibility/ dissemination, suggesting that strategies for blocking IL-1β maturation may not carry the same risks for infection as those blocking its receptor (46). These findings illustrate a paradigm in which IL-1β and the inflammasome are not functionally redundant, with implications for atherosclerosis. Therefore, strategies to block the IL-1β pathway in proximal steps such as by relieving organelle stress induced by dietary fats may be beneficial in atherosclerotic patients and bypass the unwanted infection risk associated with ablating IL-1β all together.

STUDY LIMITATIONS. Here, we showed modulation of ISR, especially by targeting eIF2B, is beneficial in atherosclerosis in mice. The feasibility of targeting eIF2B requires further testing in human atherosclerosis in future studies.

CONCLUSIONS

Targeting homeostatic pathways such as unfolded protein response (UPR) and ISR in complex diseases has been challenging, because ablating an essential stress response in a long-term fashion can have unwanted effects (such as pancreas toxicity associated with PERK inhibition) (48). Furthermore, genetic mouse models for important players in these pathways yielded confusing results through unintentional hyperactivation of other pathway components (49). Many groups have tackled this challenge by using

chemical chaperones to relieve general ER stress or small molecules targeting one of the proximal regulators in the tripartite UPR signaling (48). These in vivo studies have taught us lessons about modulating the UPR that were not predictable from cell-based studies. For example, inositol-requiring enzyme-1's (IRE1's) endoribonuclease (RNase) activity has been associated with cell survival as opposed to its kinase activity associated with death (1), but IRE1 RNase inhibitors showed their in vivo anti-inflammatory properties are beneficial by mitigating atherosclerosis (7). Furthermore, in vivo studies with small molecules to modulate key molecular players in the ISR have begun to illuminate how to fine tune this homeostatic response in complex diseases (25,39,48). In this study, using several different approaches to modulate eIF2α phosphorylation, we demonstrated ISR's causal role in lipid-induced inflammasome activation, inflammation, and atherosclerosis progression. Among these strategies, eIF2B activation (by ISRIB) appears to be the most advantageous in atherosclerosis. First, unlike PERK kinase inhibitors ISRIB is not associated with toxicity. Second, detailed mechanism of how ISRIB impacts translation was recently illuminated (36). Third, ISRIB's unique memory enhancing effects combined with its anti-inflammatory and anti-atherosclerotic actions suggest targeting eIF2B locus could combat both memory decline and CVD, especially in an aging population (27,39). Further studies are needed to illuminate ISRIB's impact on aging, but the available information on the specificity, efficacy, and mechanism of action of ISRIB suggest eIF2B could be a desirable, molecular target for the modulation of the ISR in atherosclerosis (26,39,40).

ADDRESS FOR CORRESPONDENCE: Dr. Ebru Erbay, Department of Medicine, Smidt Heart Institute & Department of Biomedical Sciences, Cedars Sinai Medical Center, 127 South San Vincente Boulevard, Advanced Health Sciences Pavilion, A9104, Los Angeles, California 90048. E-mail: ebru.erbay@cshs.org. Twitter: @CedarsSinai.

PERSPECTIVES

COMPETENCY IN MEDICAL KNOWLEDGE: Dietary fats stress anabolic and catabolic organelles and promote inflammation, accelerating atherosclerosis. Inhibition of organelle stress responses in a murine model reduces lipid-induced inflammation and slows the progression of atherosclerosis.

TRANSLATIONAL OUTLOOK: Further research should be directed toward developing methods of modulating organelle stress responses to hyperlipidemia that ameliorate inflammation and prevent atherosclerosis without the risk for infection associated with immunosuppression.

REFERENCES

1. Walter P, Ron D. The unfolded protein response: from stress pathway to homeostatic regulation. Science 2011;334:1081–6.

2. Pakos-Zebrucka K, Koryga I, Mnich K, Ljujic M, Samali A, Gorman AM. The integrated stress response. EMBO Rep 2016:1374–95.

3. Hotamisligil GS. Inflammation, metaflammation and immunometabolic disorders. Nat Rev 2017; 542:177–85.

4. Ozcan U, Cao Q, Yilmaz E, et al. Endoplasmic reticulum stress links obesity, insulin action, and type 2 diabetes. Science 2004;306:457–61.

5. Erbay E, Babaev VR, Mayers JR, et al. Reducing endoplasmic reticulum stress through a macrophage lipid chaperone alleviates atherosclerosis. Nat Med 2009;15:1383–91.

6. Thorp E, Li G, Seimon TA, Kuriakose G, Ron D, Tabas I. Reduced apoptosis and plaque necrosis in advanced atherosclerotic lesions of Apoe-/- and Ldlr-/- mice lacking CHOP. Cell Metab 2009;9:474–81.

7. Tufanli O, Telkoparan Akillilar P, et al. Targeting IRE1 with small molecules counteracts progression of atherosclerosis. Proc Natl Acad Sci U S A 2017; 114:E1395–404.

8. Zhou AX, Tabas I. The UPR in atherosclerosis. Sem immunopathol 2013;35:321–32.

9. Feng B, Yao PM, Li Y, et al. The endoplasmic reticulum is the site of cholesterol-induced cytotoxicity in macrophages. Nat Cell Biol 2003;5: 781–92.

10. Wang DD, Hu FB. Dietary fat and risk of cardiovascular disease: recent controversies and advances. Annu Rev Nutr 2017;37:423–46.

11. Sacks FM, Lichtenstein AH, Wu JHY, et al. Dietary fats and cardiovascular disease: a presidential advisory from the American Heart Association. Circulation 2017;136:e1–23.

12. Li Y, Hruby A, Bernstein AM, et al. Saturated fats compared with unsaturated fats and sources of carbohydrates in relation to risk of coronary heart disease: a prospective cohort study. J Am Coll Cardiol 2015;66:1538–48.

13. Hotamisligil GS, Erbay E. Nutrient sensing and inflammation in metabolic diseases. Nat Rev Immunol 2008;8:923–34.

14. Wang Y, Wang GZ, Rabinovitch PS, Tabas I. Macrophage mitochondrial oxidative stress promotes atherosclerosis and nuclear factor-kappaB-mediated inflammation in macrophages. Circ Res 2014;114: 421–33.

15. Çimen I, Kocatürk B, Koyuncu S, et al. Prevention of atherosclerosis by bioactive palmitoleate through suppression of organelle stress and inflammasome activation. Sci Transl Med 2016;8: 358ra126.

16. Wen H, Gris D, Lei Y, et al. Fatty acid-induced NLRP3-ASC inflammasome activation interferes with insulin signaling. Nat Immunol 2011;12: 408–15.

17. Alexander MR, Moehle CW, Johnson JL, et al. Genetic inactivation of IL-1 signaling enhances atherosclerotic plaque instability and reduces outward vessel remodeling in advanced atherosclerosis in mice. J Clin Invest 2012;122:70–9.

18. Guo H, Callaway JB, Ting JP. Inflammasomes: mechanism of action, role in disease, and therapeutics. Nat Med 2015;21:677–87.

19. Horng T. Calcium signaling and mitochondrial destabilization in the triggering of the NLRP3 inflammasome. Trends Immunol 2014;35:253–61.

20. Myoishi M, Hao H, Minamino T, et al. Increased endoplasmic reticulum stress in atherosclerotic

plaques associated with acute coronary syndrome. Circulation 2007;116:1226–33.

21. Axten JM, Medina JR, Feng Y, et al. Discovery of 7-methyl-5-(1-{[3-(trifluoromethyl)phenyl]acetyl}-2,3-dihydro-1H-indol-5-yl)-7H-pyrrolo[2,3-d]pyrimidin-4-amine (GSK2606414), a potent and selective first-in-class inhibitor of protein kinase R (PKR)-like endoplasmic reticulum kinase (PERK). J Med Chem 2012;55:7193–207.

22. Maas NL, Singh N, Diehl JA. Generation and characterization of an analog-sensitive PERK allele. Cancer Biol Ther 2014;15:1106–11.

23. Bishop AC, Ubersax JA, Petsch DT, et al. A chemical switch for inhibitor-sensitive alleles of any protein kinase. Nature 2000;407:395–401.

24. Papa FR, Zhang C, Shokat K, Walter P. Bypassing a kinase activity with an ATP-competitive drug. Science 2003;302:1533–7.

25. Das I, Krzyzosiak A, Schneider K, et al. Preventing proteostasis diseases by selective inhibition of a phosphatase regulatory subunit. Science 2015;348:239–42.

26. Carrara M, Sigurdardottir A, Bertolotti A. Decoding the selectivity of eIF2alpha holophosphatases and PPP1R15A inhibitors. Nat Struct Mol Biol 2017;24:708–16.

27. Sidrauski C, McGeachy AM, Ingolia NT, Walter P. The small molecule ISRIB reverses the effects of eIF2α phosphorylation on translation and stress granule assembly. eLife 2015;4:e05033.

28. Hori O, Ichinoda F, Tamatani T, et al. Transmission of cell stress from endoplasmic reticulum to mitochondria enhanced expression of Lon protease. J Cell Biol 2002;157:1151–60.

29. Han J, Back SH, Hur J, et al. ER-stress-induced transcriptional regulation increases protein synthesis leading to cell death. Nat Cell Biol 2013;15:481–90.

30. Thomas RE, Andrews LA, Burman JL, Lin W-Y, Pallanck LJ. PINK1-Parkin pathway activity is regulated by degradation of PINK1 in the mitochondrial matrix. PLOS Genet 2014;10:e1004279.

31. Tabas I. The role of endoplasmic reticulum stress in the progression of atherosclerosis. Circ Res 2010;107:839–50.

32. McAlpine CS, Werstuck GH. Protein kinase R-like endoplasmic reticulum kinase and glycogen synthase kinase-3α/β regulate foam cell formation. J Lipid Res 2014;55:2320–33.

33. Moreno JA, Halliday M, Molloy C, et al. Oral treatment targeting the unfolded protein response prevents neurodegeneration and clinical disease in prion-infected mice. Sci Transl Med 2013;5. 206ra138.

34. Tabas I, Lichtman AH. Monocyte-macrophages and T cells in atherosclerosis. Immunity 2017;47:621–34.

35. Sidrauski C, Acosta-Alvear D, Khoutorsky A, et al. Pharmacological brake-release of mRNA translation enhances cognitive memory. eLife 2013;2:e00498.

36. Tsai JC, Miller-Vedam LE, Anand AA, et al. Structure of the nucleotide exchange factor eIF2B reveals mechanism of memory-enhancing molecule. Science 2018;359:eaaq0939.

37. Sidrauski C, Tsai JC, Kampmann M, et al. Pharmacological dimerization and activation of the exchange factor eIF2B antagonizes the integrated stress response. eLife 2015;4:e07314.

38. Sekine Y, Zyryanova A, Crespillo-Casado A, Fischer PM, Harding HP, Ron D. Mutations in a translation initiation factor identify target of a memory-enhancing compound. Science 2015;348:1027–30.

39. Chou A, Krukowski K, Jopson T, et al. Inhibition of the integrated stress response reverses cognitive deficits after traumatic brain injury. Proc Natl Acad Sci U S A 2017;114:E6420–6.

40. Axten JM, Romeril SP, Shu A, et al. Discovery of GSK2656157: an optimized PERK inhibitor selected for preclinical development. ACS Med Chem Lett 2013;4:964–8.

41. Sheedy FJ, Grebe A, Rayner KJ, et al. CD36 coordinates NLRP3 inflammasome activation by facilitating intracellular nucleation of soluble ligands into particulate ligands in sterile inflammation. Nat Immunol 2013;14:812–20.

42. Duewell P, Kono H, Rayner KJ, et al. NLRP3 inflammasomes are required for atherogenesis and activated by cholesterol crystals. Nature 2010;464:1357–61.

43. Abderrazak A, Couchie D, Mahmood DF, et al. Anti-inflammatory and antiatherogenic effects of the NLRP3 inflammasome inhibitor arglabin in ApoE2.Ki mice fed a high-fat diet. Circulation 2015;131:1061–70.

44. Ridker PM, MacFadyen JG, Everett BM, et al. Relationship of C-reactive protein reduction to cardiovascular event reduction following treatment with canakinumab: a secondary analysis from the CANTOS randomised controlled trial. Lancet 2018;391:319–28.

45. Ridker PM, Everett BM, Thuren T, et al. Antiinflammatory therapy with canakinumab for atherosclerotic disease. N Engl J Med 2017;377:1119–31.

46. LaRock CN, Todd J, LaRock DL, et al. IL-1beta is an innate immune sensor of microbial proteolysis. Sci Immunol 2016;1:eaah3539.

47. Hsu LC, Enzler T, Seita J, et al. IL-1beta-driven neutrophilia preserves antibacterial defense in the absence of the kinase IKKbeta. Nat Immunol 2011;12:144–50.

48. Maly DJ, Papa FR. Druggable sensors of the unfolded protein response. Nat Chem Biol 2014;10:892–901.

49. Lee AH, Heidtman K, Hotamisligil GS, Glimcher LH. Dual and opposing roles of the unfolded protein response regulated by IRE1{alpha} and XBP1 in proinsulin processing and insulin secretion. Proc Natl Acad Sci U S A 2011;108:8885–90.

KEY WORDS atherosclerosis, dietary fats, inflammasome, integrated stress response, interleukin-1β, lipid-induced inflammation, metabolic inflammation

APPENDIX For an expanded Methods section and acknowledgments, as well as supplemental figures, please see the online version of this paper.